SOVIET PHYSICS USPEKHI VOLUME 12, NUMBER 6 MAY-JUNE 1970

621.385.833

SCANNING ELECTRON MICROSCOPY

G. V. SPIVAK, G. V. SAPARIN, and M. V. BYKOV

Moscow State University

Usp. Fiz. Nauk 99, 635–672 (December, 1969)

I. INTRODUCTION

THE scanning electron microscope (SEM) is an apparatus which permits samples of arbitrary geometry to be examined without special preparation and with a resolution one order of magnitude better than in optical microscopy. Its operation is based on the television principle of scanning the surface of the sample with a thin beam of electrons or ions. As a result of the interaction of the beam with the material, a number of physical phenomena are excited at each point of the surface of the sample, and registered by appropriate detectors, and after amplification, a signal from them modulates the intensity of the kinescope, the sweep of which is synchronized with the displacement of the primary beam. In this way, each element of the sample surface is in a one-to-one correspondence with the intensity of the specific point on the screen.

The magnification of the apparatus is determined by the ratio of the amplitude of the beam sweep on the screen of the kinescope and on the sample. The beam in the kinescope has significantly greater amplitude than on the sample. Although, at best, the resolution of the SEM is of the roder of 50—100 Å and is approximately one order worse than that of a modern transmission microscope, the SEM has important fields of application and capabilities rendering it, at present, an irreplaceable apparatus.

The SEM permits the direct study of massive specimens, and possesses a depth of focus of 0.6—0.8 mm, which, for example, is two orders greater than that of optical and other electron microscopes. Since the brightness of an area element on the specimen surface depends on the angle of inclination relative to the incident beam of light or electrons, the image on the screen of the microscope is automatically interpreted as a three-dimensional image. By means of the SEM it is possible to visualize both magnetic and electrical microfields, even in the case where the latter are located under a protective coating of an oxide film. Moreover, the analyzing electron probe which furthermore scans the sample, has a very small current, and the power released from an element of surface is insufficient for heating or destroying even biological specimens. This apparatus combines electron-optical and radiotechnical principles of image formation, which renders it an extremely flexible instrument and allows it to use optical as well as radiotechnical methods. In a given mode, the SEM may be used for technological operations: the preparation of photoresists, the production of local diffusion in semiconductors, micromachining and others. On return to the mode of observation, the operator can verify the results.

Reviews of the information concerning the scanning electron microscope have already appeared in print.[1-5,61] The 1965 review by Oatley, Nixon, and Pease[4] abstracts nearly 50 works, and in the present time vigorous progress of this field (at present several hundred works are already known) and its extensive use in micro- and semiconductor-electronics, in solid-state physics, biology, and others have led to the appearance of the fundamental monograph by Thornton.[5] The importance of this trend of electron microscopy is reflected in the manufacture of a large collection of commercial instruments in England, the USSR, Japan, and France (the SEM and scanning x-ray microanalyzers). The present survey is devoted to a description and to the principal applications of instruments of the former type.

An apparatus with a scanning beam was first constructed by Knoll in 1935 and served for the investigation of the change of the potential of surfaces during electron bombardment[6] and secondary emission.[7] A true SEM, giving an image "in transmission," appeared only in 1938;[8-10] the diameter of the beam was 100 Å. The recording of the image was carried out on photographic film using mechanical movement of the sample relative to the fixed beam. In 1942, an apparatus with a resolution of 500 Å working in reflection was constructed by Zworykin.[11] Davoine[12] in 1957 did not use an electron collector in the construction of his instrument, but registered the light emission produced by the interaction of the incident beam of electrons with the luminiscent material. In 1946, the first theoretical work of Brachet[13] appeared, where it was shown that, with the help of the SEM it is possible to attain a resolution of 100 Å with the condition that the radio circuit does not introduce additional noise. However, only in 1965 did Nixon and Pease succeed in constructing an SEM with an as yet unexcelled resolution of 100 Å. The diameter of the beam obtained was equal to 50—70 Å, but because of the effects of scattering of electrons in the solid body the resolution was rendered somewhat worse. (In the mode of elastically reflected electrons, a resolution of 50 ± 10 Å was obtained.[143]) In 1953, McMullen,[15] was the first to use electron intensification at a resolution of 500 Å for the registration of secondary electrons, and a double deflecting system for the primary beam was introduced to extend the range of magnification.

In 1964 in England, a commercial SEM instrument was marketed. The "Stereoscan" apparatus, which is presently in regular production (Fig. 1),[17] has a resolution on the order of 200—250 Å. The firm "JEOL" (Japan) developed two models of the SEM.[18,19] The second model of the apparatus, the "JSM-2," has approximately the same resolution as the "Stereoscan." A second Japanese firm, Hitachi, is ready for delivery of an SEM fundamentally reserved for the investigation of semiconductors.[20]

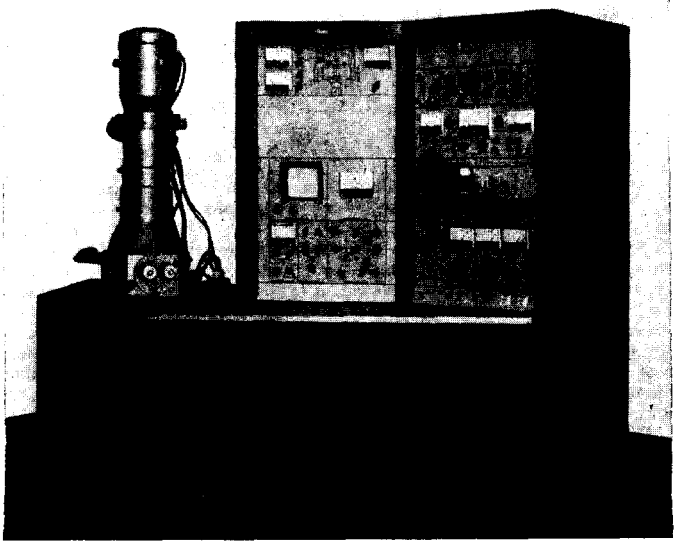

FIG. 1. "Stereoscan" SEM [17].

In the USSR, the SEM-microanalyzer (designated RÉMMA), "MAR-2" and the low voltage SEM (RÉMN) are produced.

The principle of construction of the SEM is shown schematically in Fig. 2. The beam of electrons proceeds from the cathode, 1, through a system of magnetic or electrostatic lenses, 2, 4, and is focused on the surface of the sample, 5. The collector, 6, gathers part of the electron current from the sample to form the video signal which, after intensification, 7, modulates the current in the light beam of the kinescope, 10. The synchronous deflection of the beam in the instrument and the cathode-ray tube is carried out by means of a sawtooth signal generator, 8 (3, 9 are the deflection coils).

The typical block diagram of an SEM is presented in Fig. 3. The electron beam is formed here by a system of lenses, 6, 7, and is scanned in a raster across the sample 13 by deflecting coils 11. The signal formed by the secondary electrons, proceeds to the video tubes 21, 22 after intensification. Visual observation is by means of a kinescope, the luminor of which has a long-lasting afterglow (not less than 30 sec) but a second tube with a small afterglow time serves the purpose of obtaining high-grade microphotographs.

The apparatus "JSM-2" is shown in Fig. 4,[19] and the small size RÉMN—in Fig. 5.[35]

II. RESOLUTION AND CONTRAST OF THE SEM

For an evaluation of the resolution of the SEM it is possible to proceed from the size of the cross section

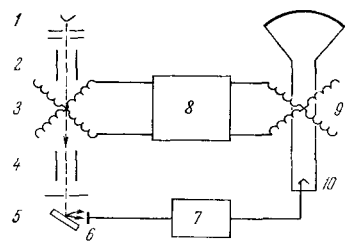

FIG. 2. Schematic Diagram of the SEM.

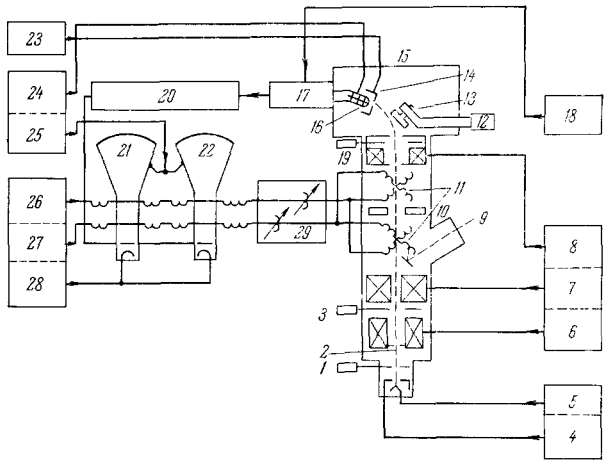

FIG. 3. Block Diagram of the SEM. 1 – anode; 2, 3, 19 – apertures; 4 – source of high voltage of 5-50 kV; 5 – filament heater; 6 – condenser lens; 7 – projector lens; 8 – objective lens; 9 – window; 10 – intermediate screen; 11 – deflection coils; 12 – specimen holder; 13 – specimen; 14 – collector; 15 – specimen chamber; 16 – scintillation counter; 17 – photomultiplier; 18 – photomultiplier power supply 1-2 kV; 20 – video amplifier; 21, 22 – video tubes for the observation and recording of the image; 23 – source of collector voltage, 400 V; 24, 25 – sources of high voltage for the scintillation counter and kinescopes, 12 kV; 26, 29 – line and frame scan generators; 28 – blanking pulses; 29 – magnification regulation.

of the electron beam being scanned over the sample. The smaller the focal spot, the greater the possible resolution, but it is necessary to take into consideration a number of factors: the discreteness of emission of electrons from the cathode, the effectiveness of the collector of secondary electrons, the aberrations of the electron-optics system forming the electron beam in the microscope, the time of scanning, and the beam current. Usually a high grade image can be guaranteed only for high levels of the signal to noise ratio. It is estimated on the basis of the shot effect, from the magnitude of thermoelectric emission from the cathode, and from the ability of the human eye to discriminate a brightness differential of not less than 5% between neighboring elements of the image. From this, the minimum number of electrons which are necessary for forming the threshold contrast can be determined. Considering also the time of scanning, we obtain the minimum permissible value of the current and the diameter of the electron beam.[4,15]

In the scanning microscope, the section of the surface whose dimensions are equal to the area of the electron spot is customarily considered to be the element being surveyed. Let n electrons fall on one element of the surface. Then the quantity $n/n^{1/2} = n^{1/2}$ determines the signal to noise ratio. We assume that the system for collecting the electrons and the signal amplification system do not change this relationship. Fluctuations in the electron current lead to a change in the brightness of adjacent elements on the screen of the kinescope, $B \pm \Delta B$. According to Rose,[21] the human eye is incapable of resolving a brightness differential so long as the signal to noise ratio does not become greater than five times the ratio $B/\Delta B$, i.e., so long as the following inequality holds

$$n^{1/2} \geqslant 5B/\Delta B. \quad (1)$$

In actual conditions, the signal to noise ratio is determined by the following factors: 1) part of the primary electrons reflected from the sample fall into the collector; 2) another part of the primary electrons is reflected from the walls of the specimen chamber; these electrons can subsequently also strike the collector; 3) the primary electrons knock out from the sample surface an equal number n_s of secondary electrons with probabilities $P(n_s)$ determined by the statistics of the secondary emission.

A decrease in the signal to noise ratio is possible also if the collector is not of high quality, when a small part of the secondary electrons is gathered. Everhart[22] and Pease[23] showed experimentally that all these factors can be taken into account in the mean and it is advisable for the calculations to use the coefficient 10 in place of 5 in relation (1).

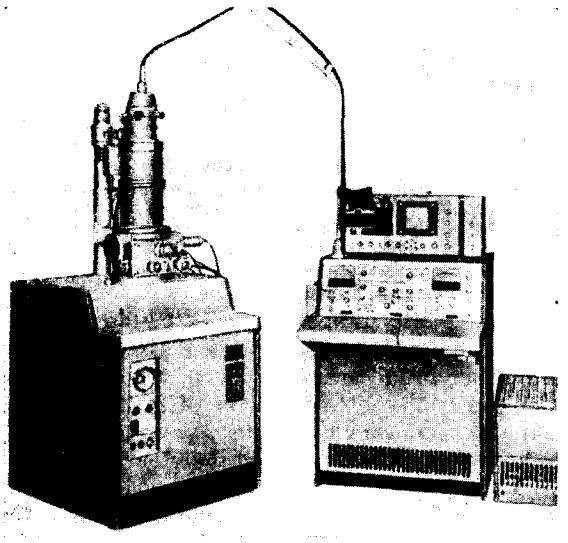

FIG. 4. SEM "JSM-2" [19].

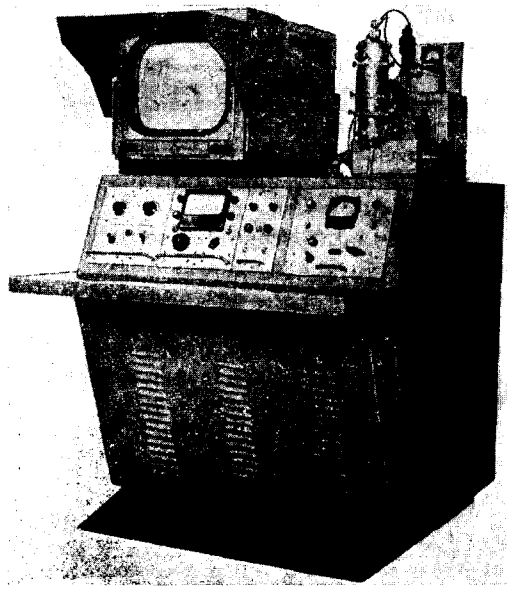

FIG. 5. Low voltage SEM (REMN) [35].

Let a square area with side D be scanned. The sweep lines formed by a beam of square cross-section, with side d_0, are adjacent to each other and subdivide the entire surface into $N^2 = (D/d_0)^2$ elements, where N is the number of sweep lines. If the beam covers the entire surface once in a time τ and the current in the beam is i, then the number of electrons per element is

$$n = i\tau d_0/D^2 e. \quad (2)$$

Using (1) and the already mentioned correction to the numerical coefficient, we find that

$$100\,(B/\Delta B)^2 \leqslant j\,d_0\tau/N^2 e, \quad (3)$$

where j is the current density of the beam in the object plane.

It is evident from (3) that a decrease of the dimension of the electron beam d_0 for improving the resolution of the apparatus must of necessity be offset by the increase in its current density, in order to guarantee, for a chosen frame exposure time and the number of scanning lines, at least if the threshold brightness contrast on the screen of the cathode ray tube.

Based on the data of Langmuir,[24] it is possible to assume that for the gun being used in an electron microscope

$$j = j_0\,(eV/kT)\,\alpha^2, \quad (4)$$

where j_0 is the current density at the cathode, V is the potential difference between the emitter and the spot where its image is formed, α is the half-angle of the beam for an observer located in the image plane. In the electron probe, the current density is not constant over the cross section and continuously decreases at the edges, following Gauss' law, as confirmed in the work of Haine.[25] Therefore, the spot diameter is conditionally determined by the boundary on which the number of electrons is one-fifth the number at the center. This spot, according to Smith,[26] contains 80% of the current.

Combining expressions (3) and (4), we have

$$d_0^2 = 100\,(B/\Delta B)^2\,kTN^2\,(j_0V\tau)^{-1}\,\alpha^{-2}. \quad (5)$$

However, the effective value of the diameter of the probe beam is determined by the total effect of the basic aberrations of the illuminating system, i.e. the, spherical (s), chromatic (c), and diffraction (f) aberrations:

$$d^2 = d_0^2 + d_s^2 + d_c^2 + d_f^2.$$

If we use the known relationships for the appropriate aberrations and expression (5), then we find

$$d^2 = P\alpha^{-2} + Q\alpha^2 + R\alpha^6,$$

where

$$P = (2{,}23\cdot 10^{-14}/V) + 100\,(B/\Delta B)^2\,kTN^2\,(j_0V\tau)^{-1},$$
$$Q = C_c\,(\delta V/V)^2, \quad R = (C_s/2)^3; \quad (6)$$

here C_c and C_s are the coefficients of chromatic and spherical aberrations. Differentiating (6) with respect to α and setting the result equal to zero, we find the value $\alpha = \alpha_{opt}$ which gives $d = d_{min}$. The expression for α_{opt} has the form

$$\alpha_{opt} = [(Q^2 - 12PR)^{1/2}/Q - 6R]^{1/4}.$$

Proceeding from these estimates, for the usual operating conditions of the SEM, it is possible to anticipate[4,15] that the resolution will be close to 100 Å regardless of whether magnetic or electrostatic lenses are used to shape the illuminating beam. Increasing τ to times greater than 5 minutes is meaningless because of the electrical and magnetic instability of the system.

In fact, the size of the spot on the sample will be larger because of the effect of surface charges on the diaphragms and of other stray electrostatic and magnetic fields. Non-coincidence of the axis of the lens and the axis of the beam also leads to an increase in the spot diameter. The unaccounted-for space charge leads to a deflection of the beam and a change of the beam form at low voltages and high current densities. The estimate of the resolution described above, based on the magnitude of the minimum contrast, gives only the value of the geometrical resolution, keeping in view the properties of the incident beam.

In a number of practical problems (p-n junctions, the structure of magnetic fields, local x-ray emission, and others) it is important, for visualization, to know both the sensitivity to microfields and the characteristics of the phenomena in the secondary emission from the sample.

The recently proposed application of the stroboscopic principle to emission,[27] reflection,[28] transmission,[29] and scanning[30-32] electron microscopy raises the question of the time resolution of the apparatus. In other words, the concept of the resolution of the electron microscope, naturally connected with the image contrast, should be extended. The resolution may be not only geometrical but also time-dependent with respect to the microfield.

The sensitivity to the microfield depends on the kinetics of the secondary electrons, and the time resolution depends on the interval of time necessary for the electron to traverse the region of influence of the microfield. The expected limit of the time resolution is of the order of a fraction of a picosecond.[30]

The contrast of the image is by no means helpful for the evaluation of the geometric resolution. Thus, for example, from the value of the microfields it is possible to estimate the magnitude of the contrast of the picture, and even to solve the inverse problem of determining those fields by measuring the contrast. These questions will be examined later.

III. LOW VOLTAGE, ION, AND TRANSMISSION SEMS

Together with the classical model of the SEM, the accelerating potential of which is 5—50 kV, instruments working at potentials less than 5 kV were constructed.[33,34] In such a microscope, the depth of penetration of the electron probe beam falls abruptly (to 100 Å), which is convenient for the study of surface films, Since the maximum value of the coefficient of secondary emission lies in the region of accelerating voltages of 500—600 V, the secondary electrons predominate in the video signal and there are practically no elastically reflected electrons which are essential for several applications. A low accelerating voltage (0.2—5 kV) introduces several problems of a physical character, connected not only with the formation of the beam, but also with the formation of the video signal. The effective wavelength of the electron beam increases and diffraction becomes perceptible. The aberrations of the lenses increase, and the resolution grows worse (0.2 μ at 1 kV). The "crossover" increases and the current density in the beam decreases.

Vertsner and Cherntsov proposed a scanning mirror (reflection) microscope.[35] The apparatus possesses an increased sensitivity to microfields, due to the fact that the illuminating electrons are slowed down by the field of the specimen. The image of a p-n junction was obtained by them at a reverse bias on the order of 0.2—0.5 V. In this very apparatus, it is possible to see the sound tracks recorded on magnetic tape. It was shown still earlier in [36a] that reflecting optics are sensitive to microfields.

Paden and Nixon[36b,c] analyzed an SEM operating mode[36b-c] in which a decelerating or accelerating electric field can act on the already formed electron beam, permitting extensive control of the energy of the primary electrons directly prior to their interaction with the specimen. This method extends the limits of application of the usual SEM and permits its use not only in the form of a low voltage SEM without the drawbacks inherent in the latter, but also in the form of an x-ray SEM with energies of the primary electrons up to 80 kV.

They analyze the questions of the formation of the electron beam and, at the same time, the influence of decelerating or accelerating fields on the electron beam. It is also shown that the beam diameter is not significantly changed. Qualitatively The problem of formation of the contrast at the new operating mode of the apparatus is considered. Experimental results of studies of semiconductors and of direct observation of the distribution of potential in the cells of the microscope grid are presented. The operation of the SEM in the transmission mode permits control of the contrast of the obtained image in a wide range.

Saparin and Spivak called attention to the fact that the use of a current of ions instead of electrons should give a marked gain in the sensitivity to microfields. The fact is that, during electron emission, the image is formed by "slow" secondary (10 eV) and fast elastically-reflected electrons. In ionic bombardment at an energy of the primary particles 30—50 eV, the secondary electrons come out from the target with a much smaller energy—only about 1—2 eV.[37] Naturally the smaller the elastic energy of the secondary electrons, the deeper their modulation by the microfields. These considerations served as the basis of the creation of a scanning ion microscope[38] (SIM), whose sensitivity to electrical microfields was shown to be 5—7 times greater than of the usual SEM. The minimum field strength to which the beam responds is estimated at 250 V/cm in the SIM and 1200—1500 V/cm in the SEM.

Recently Drummond and Long[39] reported the use of a scanning ion microscope for microelectronics, with an ion beam diameter of 1 μ. Gabbay and coworkers used lithium ions in a scanning system; the beam cross section was of the order of 3 μ.[40]

It is certain that failure to surmount the difficulties connected with ionic beams of high density, of suffi-

ciently small cross section, and of the necessary monochromatization will retard progress in the development of the SIM. However, presently, it can find application as an instrument in several problem areas of microelectronics.

Besides, it is well known that ionic bombardment is accompanied by cathodic sputtering.[41] As was shown by Castaing,[42-44] this phenomenon in the ionic microscope in conjunction with a mass spectrograph can be used for local microanalysis of the sample being irradiated.

The construction of a transmission SEM has been proposed in [45-50] In this apparatus, electrons pass through the sample and are subsequently analyzed according to their energies. The collectors of the electron current may be of the usual type—scintillators or photomultipliers. They are located at various levels with respect to the vertical, serving as pickups for a multichannel energy analyzer. The use of the multichannel spectrum analyzer with an energy resolution 0.8 eV in energy permits regulation of the contrast because the image of a selected section can be formed in any energy interval.

IV. VARIOUS PHENOMENA USED FOR THE FORMATION OF THE VIDEO SIGNAL

In contrast to the electron microscopes of the transmission, emission, mirror, and reflection types, in the scanning microscope, part of the optical system for forming the image of the specimen is missing. One of the first works on the formation of contrast was the article by Everhart.[51] Based upon his own experiments and the data of McMullen,[15] Sternglass,[52] and Palluel,[53] Everhart was able to establish that the formation of the image proceeds not only on account of the slow electrons, but also on account of the fast electrons coming from the sample. The image contrast itself depends on the atomic number, the coefficient of secondary emission of the material, the angle of inclination of the surface of the element being analyzed to the beam, the electric potential of the viewed point of the sample, etc. It was further shown that the image in the SEM may be formed similarly on account of a number of other physical phenomena accompanying the interaction of the electron or ion beam with the solid body. This is one of the remarkable properties of the SEM. In Fig. 6 is shown the variety of physical processes used for the formation of a video signal. Kimoto[54] and Wainryb and Philliber[55] showed that the image may be formed by using absorbed electrons. Everhart[56] used, for this the phenomenon of induced current in a semiconductor,

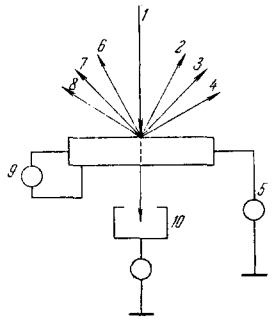

FIG. 6. Physical phenomena accompanying the interaction of an electron or ion beam with matter and their utilization in forming video signals. 1 – Electron or ion beam, 2 – secondary electrons, 3 – elastically scattered electrons, 4 – secondary ions, 5 – charges absorbed by the sample, 6 – light radiation, 7 – infrared radiation, 8 – x-radiation, 9 – induced current, 10 – charges transmitted through the sample.

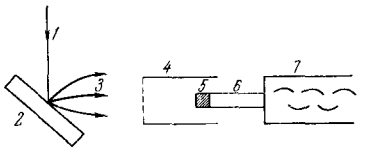

FIG. 7. Collector unit of SEM. 1 – Electron or ion beam, 2 – sample, 3 – trajectories of secondary electrons, 4 – grid held at a regulated positive potential of 400V and serving to attract secondary electrons, 5 – scintillator maintained at a high voltage of 10–12 kV and imparting to the secondary electrons the energy necessary for excitation, 6 – light pipe, 7 – photomultiplier.

Davoine and Pinnard[12,57] investigated phosphorescing samples using already emitted light caused by their bombardment with electrons. Successful studies of semiconductors in infrared illumination were made by Wittry.[58-60] It was already mentioned above that it is possible to obtain an image formed by electrons passing through a film specimen when the SEM operates in the "transmission" mode. Besides the transmission effects, there still exist local x-ray and ionic radiation which form the basis of the scanning x-ray and ion microanalyzers proposed by Castaing.[42,70]

The system of collecting the secondary electrons produced by particle bombardment is shown in Fig. 7. The field of the collector attracts electrons towards the grid. They are accelerated to energies of 6–10 kV in the interval between the grid and the scintillator, and they generate its phosphorescence which is transmitted by a light pipe to the photomultiplier to form the video signal.

Analyzing the composition of the secondary electrons, it is possible to detect the presence of slow electrons with energies up to 50 eV and fast electrons with energies from 50 eV up to the energy of the primary beam. Everhart and his co-authors[51] established that the slow electrons comprised 65% of the total current into the collector, the elastically scattered electrons—5%, and the electrons scattered from different surfaces of the chamber—30%.

By varying the conditions of the collection of electrons, it is possible to obtain an image by means of slow electrons, fast electrons, or both. The contrast with slow electrons is essentially different from the contrast with fast electrons. This is explained by the fact that the slow electrons fall into the collector along curved trajectories, whereas for the elastically scattered particles the trajectories are determined only by the angle of inclination of the specimen surface to the beam. The slow secondary electrons produce an image presence of parts that are not visible from the collector, i.e. they reflect a larger number of details of the surface than the fast electrons.

The contrast of the image in the SEM is influenced by the following basic factors:

a) Topography of the surface. In this case the contrast for fast and slow electrons is determined mainly by the angle of inclination of the element of the surface to the incident beam. For samples having a complex surface, a shadow effect occurs similar to the image in an optical microscope during oblique illumination of the surface, i.e., there exist regions not accessible to incident electron beam because of microprojections,

and consequently these places are seen on the screen as shadows.

b) Chemical nature of the sample. During scanning of a specimen with complex chemical composition by an electron beam, the number not only of secondary, but also of elastically scattered electrons may change. Knoll[7] was able to obtain contrast on account of the variation of the coefficient of secondary emission σ. When the specimen is composed of elements with slightly differing σ, the contrast is due mainly to elastically scattered electrons. With an increase in atomic number, the current of elastically scattered electrons increases.[52,53]

c) Electrical potential and magnetic field at the surface. The form of the trajectories along which the secondary electrons reach the collector is determined by the electric field strength, the magnitude of the initial speed of the electrons, and the angle of emission. Oatley and Everhart[62] indicated that the potential of the sample also plays a role in the formation of contrast. When a cutoff bias is applied to the p-region and the n-region is grounded, the latter is darker on the screen than the former. The resultant change of the initial arrangement of the equipotentials in space between the specimen and the collector will then change the current of secondary electrons, and consequently also the contrast, at a constant position of the entrance slit.

The magnetic field is also visualized in the scanning microscope.[35,63,64] Recently there has been proposed a method of measuring it.[141]

d) The current induced by the electron beam in semiconductors. During bombardment of a semiconductor by electrons, energy is transferred to the valence electrons, which move to the conduction band and, consequently, electron-hole pairs are produced. After the excitation of the minority carriers, they diffuse and recombine. If the pair production occurs near the p-n region and the pairs succeed in crossing this region, then this induced current can be registered by connecting the p or n region to an amplifier. This method, proposed by Everhart and co-workers,[56] is very important, since it allows the observation of p-n junctions under a protective film of oxide and even under a metallic film, to determine the depth of location of the p-n junction, and to study dislocations in semiconductors.[65,66]

e) Light emission. Upon bombardment of luminors by electron beams, the emission brightness is determined by the energy of the bombarding electrons and the density of the beam, and also by the dynamics of the charges arising because of secondary electron emission. The contrast of the image obtained in the emitted light is created on account of the uneven emission of neighboring elements and depends basically on the electronic excitation of the specimen, its physical structure, the time of observation, and the temperature.

f) Infrared emission. After excitation of the electronic system of a semiconductor by an electron beam, it is possible to restore it to an equilibrium state accompanied by recombination of electron-hole pairs. In this case, either visible or infrared emission is possible. The contrast of the image arises, in such a case, because of the local peculiarities of the process of recombination: the presence of a p-n junction region, inhomogeneity of concentration of impurities, dislocations, and others. For registering infrared emission, photomultipliers with a maximum spectral characteristic in the 1.0—1.2 μ range are used. Recently emission up to 4 μ was successfully registered using a semiconductor pickup made of PbS and a resonance method of increasing sensitivity.[67]

g) X-ray emission excited by the primary beam of electrons. The characteristic component of the emission is widely used for the local determination of the composition of a substance.[41b,42,68,69]

h) Ion-ion emission, as already noted above, may also be used for microanalysis of compounds.[42,70]

i) Contrast of the image formed in a transmission SEM. In this apparatus, the image is formed in the same way as in the usual transmission microscope, on account of the local scattering of electrons in different parts of the sample because of the variation in thickness and mass. The contrast of two adjacent points is determined by the difference in the number of electrons reaching the collector. A high energy resolution of the analyzer makes possible a very precise energy analysis based on the contrast of the image in a narrow energy interval.[47]

V. QUANTITATIVE TREATMENT OF THE IMAGE CONTRAST

Easiest to treat is the case when the image is formed by secondary electron emission and the object of the study is the electric or magnetic microfield. One can distinguish between two problems: the direct problem, when the microfield is given and it is required to find the contrast of the image, and the reverse problem when the distribution of microfields must be learned from the observed contrast.

Analytical and numerical calculations for a p-n junction[64,71] were conducted for the direct problem on the assumption of Gaussian distribution of the density of the secondary electrons on the surface of the collector: $j = j_0 e^{-(x/a)^2}$ where a is the distribution parameter. Under the action of a microfield, the entire distribution curve is shifted a certain distance relative to the collector slit (Fig. 8). The relative contrast K(x) is defined as the ratio of the current passing through the slit of the collector in the presence of a disturbance, to the current in the absence of the microfield. If the slit is narrow, $l \ll a$ (l is the width of the slit), then the expression for the contrast is

$$K = e^{-(2cY+Y^2)a^{-2}},$$

where c is the distance from the center of the slit to

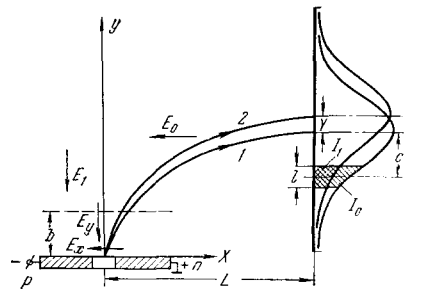

FIG. 8. Shift of the electron trajectories under the action of an electric microfield.[64]

the peak of the distribution curve and Y is the deflection of electrons under the influence of the microfield.

If $y > b$, the motion of the electron is determined by the accelerating field of the collector. The deflection of the electron in the plane of the collector was determined from the solution of the equations of motion of the electron in the regions $y < b$ and $y > b$, and, for the determination of K(x), an analytical expression is given for the distribution of the potential on the p-n junction:

$$\varphi(x, y) = (U_0/\pi)\,\mathrm{arctg}\,[x/(y+d)],$$

where U_0 is the potential difference on the p-n junction.

Several types of contrast[71a,72] were obtained experimentally earlier. The analytical calculation explains the variety of contrasts (Fig. 9), which is due both to the magnitudes of the tangential and normal components of the microfield and to the relationship between the micro- and macrofields (E_x, E_y, and E_1, E_0).

A numerical calculation showed how the type of contrast changes with changing accelerating field, with the bias applied to the sample, and with the position of the slit. These changes of contrast are caused by the shift of the Gaussian distribution curve relative to the slit of the collector.

It is possible to observe not only electric but also magnetic microfields. Electron-optical visualization of magnetic microfields was first accomplished in the emission microscope[75] and later in the electron mirror microscope.[76] With the help of a low-voltage SEM, Vertsner and Chentsov[35] succeeded in producing an image of a magnetic recording, but Banbury and Nixon[63] were successful in visualizing domain structure by means of a usual SEM. In [65], the modulation of the video signal was used for the observation of weak magnetic fields. The contrast of the image of a magnetic field of a sound-recording head was determined numerically[64] (Fig. 10).

The solution of the inverse problem—finding the distribution of an electric microfield from its contrast—

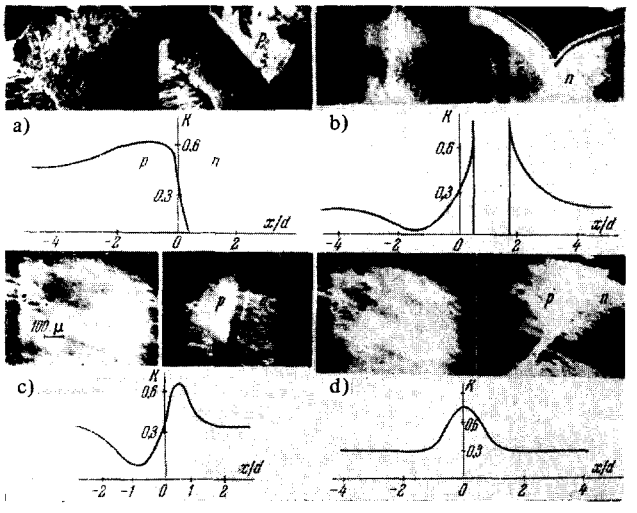

FIG. 9. Types of contrast of the image of a p-n junction [71a]. Above are the experimental photographs (at the left, without an applied inverse bias, at the right, with a bias). Below is the calculated contrast distribution.

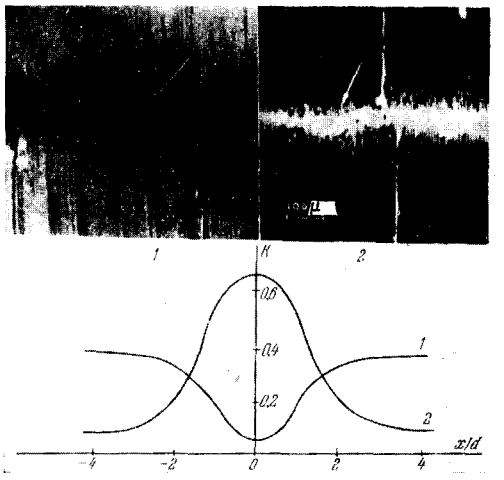

FIG. 10. Two types of contrast in the region of a non-magnetic gap [64]. The regions of the magnetic field are shown by arrows. Below are presented the theoretical contrast curves.

can be found if the field intensity of the collector is sufficiently high and the dimensions of the microfield are small.

As to the distribution function of a microfield φ', it is necessary to solve the integral equation

$$S(x) = \left(\frac{m}{2E_0 e}\right)^{1/2} \int_0^l \frac{\dot{x}(\xi)\,d\xi}{\sqrt{\xi}} = \frac{(l/2)^{1/2}}{E_0} \int_{-\infty}^{+\infty} \frac{\varphi'(x-\xi)}{|\xi|^{1/2}}\,d\xi.$$

Such a solution is obtained by the method of Fourier transformation[77] and has the form

$$\varphi'(x) = \frac{E_0}{2\pi(2l)^{1/2}} \int_{-\infty}^{+\infty} \frac{S(x) - S(x-\xi)}{|\xi|^{3/2}}\,d\xi;$$

here S(x) is the displacement of the electron in the collector plane under the action of a microfield, l is the distance from the collector plane to the specimen, and E_0 is the external field. If the function S(x) is known, the distribution $\varphi'(x)$ as well as $\varphi(x)$ can be found with an electronic computer. One must, however, bear in mind that the task of solving the inverse contrast problem is an incorrectly stated problem. If the experimentally determined function is not sufficiently smooth, then the regularization method of Tikhonov must be used (see [78]). Similar calculations were carried out also for the solution of the inverse problem for a magnetic field:

$$B_{0x} = \frac{1}{\pi}\left(\frac{mE_0}{2el}\right)^{1/2} \int_{-\infty}^{+\infty} \frac{S(x) - S(x-\xi) - \xi S'(x)}{\xi^2}\,d\xi.$$

Experimental determination of electric and magnetic microfields was conducted[79] with an SEM of the "Stereoscan" type, in which several small changes of the collector assembly had been made.

VI. INCREASE OF THE SENSITIVITY OF THE SEM

The intensity of the video signal is determined by: (a) the scatter in the velocities of the secondary electrons, (b) by the ratio of the intensity of the microfield to the macrofield accelerating the electrons,[80] and (c) by the noise of the system.

In the SEM working in the reflection mode and at low accelerating voltages, (a) and (b) are favorable

factors. Noise is still present in the system, thus limiting the sensitivity to microfields. In the usual SEM, where the scatter of secondary electrons is large, all three factors are harmful.

The possibility of increasing the sensitivity relative to the background noise was demonstrated in [82,84]. This corresponds to Nyquist's theory, according to which the signal to noise ratio can be increased by decreasing the bandwidth of the video amplifier. To this end, one uses the principle of modulation of the signal by the studied microfields.

Use of this method also makes it possible to obtain an image not only of a dc but also of an ac magnetic microfield.[81]

For observation of ac magnetic fields, one uses the modulation principle of selective intensification of the video signal in a narrow band of frequencies. A magnetic recording head served as a source of the magnetic field, and the field in its gap was excited by an alternating current. The surface video signal formed by the secondary electrons was mixed with a signal having a definite carrier frequency from regions where an alternating magnetic field exists. To amplify and separate the field signal, it is fed to a resonant amplifier tuned to the used modulation frequency. In this way, regardless of the noise of the system, it is possible to observe a small magnetic field. The frequency of the current exciting the alternating magnetic field is selected such that many pulsations of the field occur during the time of motion of the electron beam across the non-magnetic gap region.

The field region is separated in the form of a light (or dark) stripe (see Fig. 10). Oscillograms of the field signal, obtained with a single sweep of the beam across the gap, have a resemblance to the distribution of horizontal component of the magnetic field strength in the gap. This confirms the proposition that the contrast of a magnetic field in the SEM is formed basically because of the horizontal components of the magnetic field.[83] It is possible to apply the principle of modulation also for the observation of constant magnetic microfields, again using resonant amplification of the video signal. The electron beam, modulated by a sinusoidal or pulsed voltage and illuminating the sample, forms a high frequency video signal modulated at low frequency by the signal from the surface of the sample. The frequency of modulation of the beam will be the carrier frequency. The circuit of the amplifier and discriminator of the low frequency signal includes the tuned amplifier and the detector. The choice of frequency of modulation of the beam is connected with the time of scanning and the dimensions of the observed inhomogeneities.

Let us assume that $\Delta\tau$ is the time in which the beam crosses the region being studied on the sample, and τ is the duration of the modulating pulse with an off-duty factor 2. In this case the following modes of operation are possible:

1) if $\tau \gg \Delta\tau$, the information concerning the inhomogeneity will be contained in the limits of one pulse, and it can not be transmitted because of the narrow bandwidth of the amplifier;

2) if $\tau \approx \Delta\tau$, the inhomogeneity is weakly revealed and details are lost;

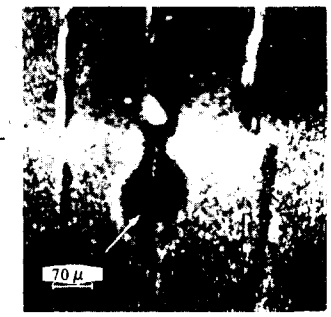

FIG. 11. Inhomogeneity of the magnetic field of a magnetic recording head (indicated by the arrow) [71b].

3) when $\tau \ll \Delta\tau$, the inhomogeneity can be clearly revealed.

Thus, to choose the minimum value of the modulation frequency it is necessary to know the approximate dimensions of the investigated inhomogeneity, in the given case—the frequency of the microfield. An estimate shows that $f_{mod} \gg f_{sc}\mathscr{L}/\delta$ where $\mathscr{L}$ is the dimension of the screen, and δ is the dimension of the inhomogeneity in the sample. In Fig. 11 is shown a display of an inhomogeneity of the magnetic field of a magnetic recording head.[71b] The maximum field strength that could be registered is 150 Oe. The contrast of the image of a magnetic field agrees with the calculation given in [83].

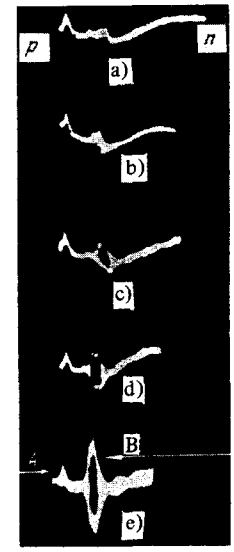

FIG. 12

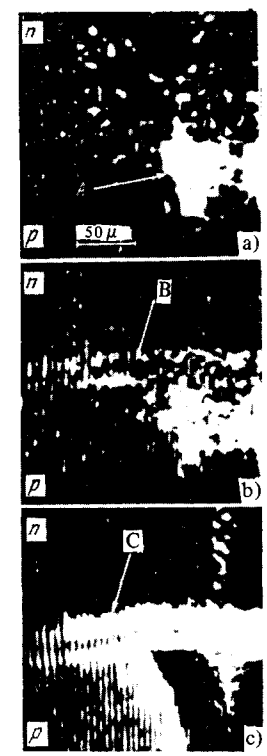

FIG. 13

FIG. 12. Oscillogram of a video signal from a p-n junction upon application of an alternating bias (with frequency 1.07 kHz)[82,84]. a) U_b = 0, b) U_b = 5 mV, c) U_b = 30 mV, d) U_b = 50 mV, e) U_b = 100 mV. Shown by arrows are: A – the signal from the geometry, B – the signal from the p-n junction.

FIG. 13. Silicon alloy diode: the photograph was obtained by means of the modulation method (frequency 1.07 kHz) [82,84]. a) U_b = 0, b) U_b = 25 mV, c) U_b = 250 mV. Shown by arrows are: A – the signal from the surface, B and C – the signals from the p-n junction.

The same method can be used for observations of extremely weak electric microfields. A periodic signal is applied to a p-n junction in place of a dc bias.[82] The secondary electrons reacting to this field, introduce an alternating component into the video signal, and the amplifier is tuned to the same modulation frequency. Since the voltage in the semiconductor diode is concentrated mainly in the region of the p-n junction, the alternating field acts only in the region of the junction. The oscillograms of Fig. 12 were taken with a single line scan of the beam across the p-n junction. In the left part is seen seen the triangular impulse from the edge of the specimen; its value is not changed with a changing amplitude of the alternating voltage. The pulse in the center oscillogram corresponds to the p-n junction region, but its appearance is noted already registered when only 10 mV is applied to the specimen.

It is possible, because of the high sensitivity and of the tuned amplifier, to obtain also an image of the p-n junction at low applied voltages. In Fig. 13b, a periodic bias of 25 mV is applied to the diode. For comparison, microphotographs of the p-n junction are given for no bias (Fig. 13a) and for a 250 mV bias (Fig. 13c). Application of the described method allows the sensitivity to electric microfields to be stepped up by two to three orders of magnitude.

It is possible to apply the resonance method also when the SEM operates in the induced current mode. In this case, the sample is irradiated by an impulsed electron probe, and the signal from the sample is applied to a tuned amplifier; this procedure also gives a sensitivity gain of one-and-a-half to two orders of magnitude.

VII. APPLICATIONS OF THE SEM

1. Technique of Amplification of Contrast

Kimoto et al.[85] describe a method using two pickups A and B, positioned at an angle to the sample and symmetrical to the beam. The sample is arranged normal to the incident current of electrons, and its surface may be observed by means of elastically reflected and absorbed electrons. The contrast will depend not only on the topography but also on the chemical composition of the substance. It is impossible to separate these two effects by the usual methods. A method of observation by means of two pickups resolves this difficulty. In one case, both pickups A and B receive an identical signal, if the signal is determined by the atomic number of the element. In the other case, the video signals from A and B are in anti-phase if they are determined by the laws of elastic scattering of electrons from inhomogeneities of the microtopography. Adding the signals, it is possible to exclude the effects of the geometry and to amplify the effect that is determined by the nature of the sample. Subtraction yields the opposite picture—the relief of the image is emphasized and the signal connected with the chemical composition of the element vanishes.

2. Technique of Stereoscopic Microtopography

Smith[86,87] and Stewart[16,88] developed a method of obtaining stereoscopic photographs. In the first method the sample is inclined to the scanning beam and the glancing angle is close to 30°. We see this surface on the screen as if we were looking along the electron beam. Therefore, in order to obtain a stereo pair, it is necessary to change the inclination of the sample by 2—15° between two successive frames. The exact angle is selected experimentally for the best three-dimensional effect.

The second method uses the rotation of the inclined sample about an axis normal to the specimen surface. To obtain a stereo pair in this case, the angle of rotation of the sample should not exceed 10° for adjacent frames. An adequate analysis of the stereo image can yield quantitative estimates of the microtopography. As the investigation of Wells[89] showed, for these purposes, the technique of preparation used in aerial photographs is applicable. This method is especially effective for the investigation of rough surfaces such as cleavages in crystals, fractures during tension of metals, porous surfaces, etc.[90]

3. Insulators

In the observation of specimens with poor conductivity at beam electron energies of 5 kV and higher, in spite of the weak beam current of 10^{-9}—10^{-12} A, the surface becomes charged. Regions of local charge appear on the screen in the form of bright clear spots of arbitrary shape and size. There exist two means of eliminating the charge.

a) The surface of the specimen is covered with a thin layer of metal. For this method, films of Al or Au deposited by thermal means to thicknesses of 300—400 Å are customarily used. After such preparation of the sample, the observation of the surface is possible even at high energies of 25—30 kV. This method is widely used in the scanning microscope for investigating such samples as synthetic fibers, biological specimens, ceramics, particles of cements, etc. However, the method described has two disadvantages. In observations of surface phenomena under conditions of deformation, the deposited layer, as shown in the dissertation of Wheeler in 1957, becomes broken and peels off from the surface. The second drawback is that there are samples on which it is impossible or very difficult to deposit a layer without harming them. Basically this applies to specimens of biological origin maintained at low temperatures.

b) The other method provides for the reduction of the accelerating potential of the beam until the coefficient of secondary emission becomes equal at all points of the scanned surface. For the majority of insulators, this is correct for electrons with energies from 1 to 2 kV and does not depend on the angle of inclination of the surface to the beam. The contrast is determined only by the topography and the location of the collector of electrons.[33,34] It was shown that such a method gives satisfactory results in the investigation of cleavages, of two-component ceramics, of dust particles, and of other dielectric materials. The observation of the structure of water vapor condensed at −190°C from room-temperature atmosphere and also of several biological specimens are interesting. Special investigations of ceramics[91] and cement[92,93] were also carried out by the described methods.

Using a high-voltage SEM (25—30 kV), it is possible

to observe the effect of charging the surface of the dielectric and the dynamics of the surface flow of charges.[94]

4. Organic and Synthetic Fibers

The SEM opens up new possibilities in the investigation of such samples as fibers of all possible origin, metallic filaments, thin spinnerettes, etc. In the majority of cases it is impossible to take replicas of surfaces of the enumerated materials for analysis of the topography with high resolution. Therefore the SEM with its large depth of focus and the possibility of observing the microgeometry of the surface without special preparation, becomes, in these cases, the only applicable instrument. However, a correct understanding of the morphology of surfaces demands the additional investigation of thin microscopic sections at high resolution in a transmission electron microscope. For the observation of orlon filaments,[95] the influence of the die shape was studied. Smith[26] carried out an investigation of wool fibers. The scaly nature of the surface appeared very well and is, as he feels, connected with the peculiarities of natural growth. In the latter of his works[95-97], and also in the work of Washburn,[98] an investigation of the fibers of Canadian spruce and the influence of the methods of drying the cellulose on the quality of the paper are described. Culpin and Dunderal[99] investigated the fracture in bending of both synthetic and cotton fibers. The image of synthetic thread is shown in Fig. 14.[100]

5. Cathode Luminescence

The alkali halide compounds KI, NaCl, LiCl, LiF, KCl, and KBr were studied in the form of crystals or sputtered films. The apparatus can study the local light emission occurring at each moment of time during illumination by the electron beam. The registration is by photomultipliers with maximum spectral sensitivity in the 2500—12,000 Å range. Besides, the investigation used the secondary-electron image with the purpose of comparing both pictures and determining the influence of topography of the surface on the distribution of centers of light emission. The following basic investigation methods are possible: a) the study of the emission spectrum, b) the influence of the duration and intensity of electron bombardment on the light emission, c) the dependence of the emission on the luminor temperature. The spectral distribution of the light emission could be successfully studied by employing calibrated filters between the specimen and the photomultiplier. In this manner, the presence of maximum emission from the luminor was established. Independently, this phenomenon was verified by the method of spectral analysis. It was noted that the change of the light emission depends on the energy of the incident electrons, i.e., on the depth of penetration, on the structure of the luminor (single crystal or film), and on the total time of observation. Reversible relaxation of the illumination sets in at accelerating voltages within the limits 5—10 kV and at medium current densities. The explanation of the described phenomena is based on the formation, in the crystal lattice, of two types of defects as a result of the bombardment of the sample: temporary (free electrons, holes, etc.), the lifetime of which is less than 10^{-5} sec, and permanent (interstitial atoms, formation of new centers, ion vacancies, etc.).

FIG. 14. Microphotographs of a synthetic fiber (nylon) at different magnifications [100].

The temperature influence on the light emission was investigated at a change of temperature of the specimen substrate from 9 to 450°K. It was ascertained that cathode luminescence of alkali halide luminors is very sensitive to a change of temperature and a decrease in emission is observed at high and low temperatures. Upon change of temperature, the reversibility of the effect is noted. The interpretation of the results is based on the band theory.

The results obtained for the emission of cadmium sulfide are interesting. In the SEM, it was successfully established that individual grains of the luminor can give red and green emission simultaneously, whereas others give only green. Lowering or raising the temperature of cadmium sulfide is accompanied by amplification or attenuation of the red emission, respectively. A change of current density toward lower values leads to a relative increase of the share of the red emission in the spectrum.[12, 57, 100-105]

6. Determination of the Atomic Number of an Element

This may be done by estimating the current passing through the sample and for the formation of the image. This current is equal to the current of the probe I_p from which the currents comprising the elastically scattered electrons I_e and the secondary emission I_s are subtracted. The latter may be diverted back to the sample if a grid having a negative potential is positioned over the sample. The number of elastically scattered electrons is determined by the atomic number of the element on which the electron beam falls at the given point, and it increases monotonically with increasing atomic number Z. In such a way, the contrast will be completely due to the local distribution of elements with different values of Z.[106]

At a geometrical resolution of 1000 Å, owing to the good stabilization of the current of the electron beam,

a resolution of the atomic number $\Delta Z \leq 0.07$ was obtained for Z = 30. Such a sensitivity made it possible to distinguish in a Cu-Zn compound the ϵ-phase with Z = 29.835 and γ-phase with Z = 29.635 and to distinguish in a Ni-Fe alloy the levels with Z = 26.93 and Z = 26.72.

A similar method was used in [107] for Fe-Si and Fe-C alloys with supplementary use of secondary emission. The video signal in this experiment was a pulse, the amplitude of which was determined by the atomic number of the element, and the shape of the peak was determined by the secondary emission.

7. Investigation of Processes of Thermal Decomposition and Oxidation. Cathode Sputtering of Metals with Oxidized Surfaces. Fatigue and Fracture of Metals and Alloys.

The decomposition of silver azide is of great interest in the study of explosive substances. Preliminary investigations with a transmission microscope and an electronograph did not give a clear representation of the chemical transformations occurring during a change in temperature. By means of the SEM,[108] this problem was successfully resolved. A needle-shaped sample of silver azide was fastened by one end to a heated metallic plate, the temperature of which would be changed in the process of observation. The resultant temperature gradient along the crystal presented an opportunity to study, in detail, all phases of thermal decomposition of the material.

In Cambridge (England), Pease et al.[14,109,110] were successful, using apparatus with resolution close to 100 Å, in following the oxidation of pure iron (0.010 C and 0.60 O) and of the "Armco" iron alloy. The specimens were subjected to electropolishing, rinsing, and afterwards oxidation in air at atmospheric pressure at a temperature of 500°C. The observations were conducted each time after each oxidation treatment. The appearance of a coarse oxide layer and the sprouting of "whiskers," the conical base of which resulted in a thick layer of a depth of the order of 0.25 μ, were noted, and the dimension continuously increased with increasing time of oxidation. The irregularities of the oxide layer after 5 minutes of oxidation were of the order of 2000 Å, and the dimensions of the "whiskers" —several hundred Angstroms. In the investigation of the "Armco" iron, it turned out that the thickness of the oxide layer and the growth of "whiskers" depend on the orientation of the iron grains. For pure iron, this effect was not observed, but the sprouting of "whiskers," as established, was connected with the locations of surface contaminations.

For the investigation of the results of ionic etching of the surface, the high-frequency ion source was installed in the specimen chamber of the SEM, and gave a current of positive 5-kV argon ions.[111] With such a construction, the mode of observation alternates with the process of etching the specimen. A possibility of combining these modes was found. The collector of electrons, in this case, was oriented in such a way that the image was formed only of fast electrons, since the ion beam creates both negative ions and slow electrons causing a strong background. Such an experiment permits the observation of the dynamic process of etching of metal in this apparatus.

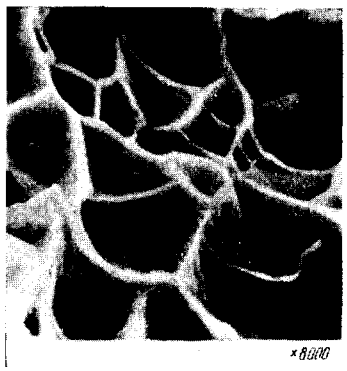

FIG. 15. Fine structure of a fracture of stainless steel (13% Cr) [100].

In metallurgy, the SEM may be used also for the studies of fatigue failure of metals, of fractures and of cracks occurring during tension, compression, torsion, etc. In Fig. 15 is shown the fine structure of a fracture of a specimen of stainless steel.[19] The work of McGrath and co-authors[112] demonstrates such possibilities of the microscope on samples of copper and aluminum alloys. These materials were subjected to cyclic deformation with a stress of $\pm$ 7000 kg/cm^2. The irreversible shearing processes arising during this deformation lead to fatigue failure. The accumulation of local residual stresses leads to the appearance of a network of microcracks which develop into cracks of macroscopic scale. Such a process leads subsequently to progressive failure of the material.

In [113] are presented the results of observation of the work of graphite crystals in Fe-C and Ni-C alloys.

8. Observations of Dislocations

By means of the SEM a comparative observation was carried out, with secondary electrons, of germanium crystals etched in CP-4 and grown under different conditions.[114] One of them was grown by the method of oriented crystallization along a [100] axis, and the other was pulled from the melt. The dislocation formations in the first crystal had the form of a series of cone-shaped knots. In the second case, little pits of different diameters and depths were observed. The authors propose that such selectivity of etching may be connected with a variation in the local concentration of electrons and holes, with the presence of regions of space charge, and with the presence of impurities. Czaja and coworkers[65,66] developed a method of analysis of dislocations in an SEM that used, together with the secondary-electron image, the image caused by the induced current. This allowed the observation, in GaP and Si samples, of p-n junctions and even individual dislocations close to the junction and simultaneously with it. The authors maintain that edge dislocations in strongly doped silicon of the n-type can be revealed by means of the induced current because of the enhanced-recombination in this region of injected carriers. Besides revealing the dislocations arising because of heat treatment and plastic deformation, the figures of the separation of oxygen in the crystal were successfully observed. A dislocation chain and detached loops were

disclosed by the method of induced current by Davies et al.[115] in mesadiodes of low-resistance silicon. The dislocations passed through the p-n junction from the p-region to the n-region. By means of the microscope it was possible to see the region of leakage upon application of a bias, just at the point of intersection of the junction and the dislocation chain. It was thought that volume and surface scattering of the electrons, selective absorption, enhanced recombination, and capture play a greater or lesser role in the formation of contrast in regions with crystal lattice defects. The dislocation chains are also described in the work of Lander.[116a]

Frequently, during the study of different types of samples, the demand for cooling them necessitates the application of special constructions which make the investigations much more difficult and expensive.

It is necessary to call attention to a procedure[116b] allowing the study of several samples without the application of a refrigeration stage. The authors were able to obtain an image of crystals of ice, which was thermally insulated in the specimen chamber and its low temperature was maintained constant owing to the small speed of sublimation of ice in vacuum. A piece of frozen clay was used as another sample.

The method described is also useful for the investigation of biological specimens. In this case, it becomes possible to compare the observed structure with that obtained upon refrigeration of a dessicated specimen.

9. Cathodes

The investigation of cathodes of different types in transmission optical microscopes is made difficult by the circumstance that their surface in the operating condition has a high temperature and has a coarse structure. Besides, it is impossible to study the different stages of the activation process, since this inevitably calls for exposing the cathode to air, a fact that, naturally, alters the true picture. The enumerated difficulties were successfully bypassed by the application of the SEM. Beck and Ahmed[117] described the results of an investigation of the process of activation of a tungsten-aluminate impregnated cathode in vacuum of 10^{-6} Torr at a geometric resolution of 200 Å. In order to get rid of the light emission falling into the photomultiplier during heating of the cathode, they used interference filters in front of the photomultiplier, and they covered the light pipe and the scintillator with a thin layer of silver. Haas and Thomas[118,119] determined the work function of uranium carbide. The work function of the "spot" region was estimated; data were obtained on the change in work function for a nonactivated surface in the process of activation and, subsequently, for constant operation of the cathode over the course of three weeks. An automatic recorder traced out the curve of the retarding potential, and from these it was already possible to judge concerning the variations in the work function. The results showed that prior to activation the dispersion of the work function in the region of the "spot" fluctuates in the interval from 3.25 to 4.5 eV. The process of activation sharply decreases the interval and $\Delta\varphi$ = 3.0—3.25 eV, the activated surface being very sensitive to the surrounding gases and may be easily contaminated.

10. Investigation of p-n Junctions

The possibility of visualizing the presence of a potential difference between the adjacent regions of the sample is one of the most interesting features of the apparatus. The first reports were published in 1957 by Oatley and Everhart,[62,120] and concerned the observation, by means of secondary electrons, of a potential difference of 4 V between the p and n parts of a silicon diode. In this case the p region appeared light on the screen, and the n region dark. Later on, other types of contrast[64] became known.

In a subsequent article,[51] the reason for the occurrence of a black-white contrast is explained by the fact that the trajectories of the slow secondary electrons and, hence the current in the collector, strongly depend on the potential of the sample. A detailed investigation of possible factors influencing the contrast of a p-n junction (the potential of the collector, the potential of the sample, the inclination of the sample relative to the beam, the distance between the sample and the collector), led to the conclusion that even a difference of potential of 0.5 V will produce a visible contrast.

Attempting to explain the nature of the contrast of the image of a p-n junction, Drummond, Thornton, and Culpin[121,122] established a map of the distribution of equipotentials in the optical photograph of the investigated section of a p-n junction in high resistance silicon (10^8 ohm-cm). They then compared this section with the electron micrograph obtained with a bias up to 500 V. It turned out that the contrast depends on the position of the collector and the diaphragm, the brightness of the image depends to a large degree on the tangential component of the electric field at the point, and not on the absolute value of the potential. The resolution over the field was estimated at 200 V/cm in a region of 4×10^{-3} cm. The use of a video signal in the form of a beam of electrons absorbed by the sample and of the current induced by the beam also allowed the detection of the location of the p-n junction and the acquisition of additional data concerning it.

Kimoto in his work[54] demonstrates the application of all possible methods (secondary emission, current of absorbed electrons, current induced by the beam) for the observation of p-n junctions in silicon.

The application of the method of absorbed electrons is described in [35]. A low voltage SEM, working at accelerating voltages from 500 to 2000 V, was constructed. It can also operate in the reflection mode. Such a mode results in a sensitivity of 0.2 V to the potential relief on the surface of the specimen.

The work of Davis et al.[115] was dedicated to an investigation of defects produced in silicon samples during the technological working. By means of secondary emission and of the current induced by the electron beam, the leakage paths in a p-n junction were successfully detected for different bias values from 0 to 12 V and were connected with dislocations and mechanical stresses. By means of the method of induced current, the internal defects of the material are very well localized. This is clearly demonstrated in a photodiode of high-resistance material.

The series of interesting investigations performed in Thornton's laboratory (North Wales, England) is devoted to a comprehensive study of p-n junctions. In a

report, Shaw, Hughes, Neve, Sulvey, and Thornton[123] examined the cause of operating failure of a GaAs semiconductor. The induced-current method revealed non-uniform diffusion and the formation of narrow and complex-shaped diffusion channels, connected in turn with the structure of the material, but not with the quality of the surface. Crystals operating well in a laser did not have such deviations in the diffusion region.

Neve, Hughes, and Thornton[124,125] conducted investigations for the clarification of the nature of the microplasma in the mesadiodes, formed by diffusion of phosphorus into p-type silicon (with a resistivity of 0.2—10 ohm-cm). By comparison of the results obtained in the optical microscope and in the SEM, at different values of the sample bias, they successfully revealed the region of localization of cascade breakdown. The authors believe the microplasma to be caused by the region of the microcracks, defects connected with surface impurities, and microfields originating in the regions of formation of small pits on the surface. Spivak, Saparin, et al.[38,73,74,84] described new types of contrast obtained during observation of semiconductor diodes of different types. Besides the well known image of an electric microfield of a p-n junction in the form of a light field by Oatley and Everhart, images were obtained in the form of a light streak, a dark streak, and a light and dark streak arranged in a row, a dark streak bordered by a light one, etc. The results of an observation of p-n junctions in an SIM are described. By means of this equipment, one of the aforementioned new types of image contrast was obtained, namely a dark streak bordered by a light one. A detailed examination of the electron trajectories, serves as the basis of an interpretation of the observed types of contrast of p-n junctions[63,64] (see also Fig. 9).

In [82], a modulation method of investigation of p-n junctions is proposed, which increases the sensitivity of the scanning microscope to microfields by 2—3 orders in comparison with all methods known earlier.

a) Quantitative observations in semiconductor electronics. For the purpose of quantitative analysis, it is possible to use almost all modes of operation of the apparatus: secondary electron emission from the surface of the specimen, the method of induced current, and emission from the surface of the sample.

For the formation of the video signal in the method of induced current,[56] a photoconduction signal is used, i.e., the voltage due to the currents induced by the electron beam (pair production) in a resistor that is external to the tested circuit and is connected between the circuit and ground. It is possible to obtain different quantitative estimates by recording the induced-current signals as functions of the change in the condition of operation of the apparatus. The essential feature of the method is that it can plot induced-current curves at any characteristic point on the surface of the specimen, i.e., it can relate the quantitative data at this point with the microphotograph.

The usual method of estimating diffusion lengths from the induced-current curve obtained for a single line scan of the electron beam through the junction—is to measure the distance from the p-n junction to the point where the current is equal to 1/e of its maximum value.[126-128] Since the induced current is given by $I \sim e^{-x/L}$, where x is the coordinate and L the corresponding diffusion length, it is possible to determine L more accurately from the graph of the linear dependence of the logarithm of the induced current versus the coordinate.

By means of this method, it is possible to measure a very short diffusion length ($L \ll 1\,\mu$) and to observe its local variations. After the measurement of the diffusion length L at a known coefficient of diffusion D, it is easy to calculate also the lifetime τ from the equation $L = (D\tau)^{1/2}$.

An original method of display and investigation of p-n junctions was proposed by Wittry.[58,59a] The electron beam scanning the semiconductor surface produces electron-hole pairs. Their recombination leads to recombination emission, Augur processes with a transfer of energy to the free carriers, and other effects. Not using secondary electrons, but registering only infrared recombination emission, the author was successful in localizing the p-n region. Since there is no recombination in the region of the p-n junction, this part is portrayed by a dark streak on the background of the remaining image. From the width of the streak, knowing the mobility, it is possible to evaluate the length and the lifetime of the minority carriers. This method was compared with the results obtained by measurement of the induced current through the same p-n junction. The author feels that the method of cathode luminescence is more accurate for the determination of small values of diffusion length than the induced-current method. By carrying out comparison measurements of the induced current at different accelerating voltages and biases, it is possible to estimate the mean value of the energy for the formation of an electron-hole pair.

Demidov and Gurova,[59b] observing the emission of a p-n junction in gallium arsenide during the interaction of the electron beam with the semiconductor, obtained several quantitative estimates of the processes occurring in the p-n junction. The image of the sample was produced simultaneously by means of secondary electrons and infrared emission with a wavelength greater than 0.7 μ. Besides, an oscillogram of the induced current was obtained. Also, the sample was cooled to 77°K.

It was possible to observe the different tendency to cathode luminescence of samples prepared on the basis of n-type gallium arsenide. This tendency depends on the structural homogeneity of the material, on the uniformity of the distribution of impurities, and on the surface structure of the specimens. An investigation of the emissivities of p- and n-regions has shown that the intensity of emission of an n-region is greater than of a p-region, a fact explained by the lesser structural perfection of the latter.

It should be noted that Thornton et al.,[129] in a lifetime calculation based on the induced-current method, obtained too low a value τ_n, possibly because of a number of reasons. In particular, the nearer to the junction the carriers are produced, the greater the diffusion length. It is just this increase of diffusion length close to the p-n junction which leads to a sharp increase in

the observed signal as soon as the primary beam approaches the junction. When this signal is interpreted by means of the diffusion length, disregarding the strong field near the p-n junction, a small value of the diffusion length is obtained, and consequently an incorrect value of the lifetime.

Another reason is the possibility of the fact that it is more readily the surface rather than the volume lifetime which is measured. The difference between these two lifetimes was also noted in [132].

By means of the scanning electron beam, it is possible to estimate the concentration of acceptor impurities.[131] The width W of the depleted region of the p-n junction is measured as a function of the applied voltage. When the inverse bias increases, the depleted layer broadens:

$$W = (2\varepsilon/eN_a)^2 (V - V_{diff})^2,$$

where ϵ is the dielectric constant of the semiconductor, N_a the concentration of the acceptor impurity, V the applied voltage, V_{diff} the diffusion potential, and e the charge of the electron. Consequently, it comes down to the determination of the change of the width of the depleted zone. It is necessary to know this change of width with a large degree of accuracy, using for this purpose sections and operating the SEM in the secondary-emission image mode.[131] It is also possible to use either the induced-current method or emission single line scanning.[132] The use of the induced-current method for the determination of the width of the depleted zone is the most exact technique, and the data obtained by this method are in good agreement with the capacitance method.[129]

In Fig. 16 is presented the dependence of the width of the depleted zone on the applied voltage. From the slope of the curve 1 it is possible to determine the concentration of acceptor atoms, $N_a = 5 \cdot 10^{13}$ atoms/cm^3. The result agrees with the data obtained by the four-point-probe method ($N_a = 4 \times 10^{15}$ atoms/cm^3). Curves 2 and 3 correspond to concentrations N_a equal to 10^{13} and 10^{14} atoms/cm^3, respectively.

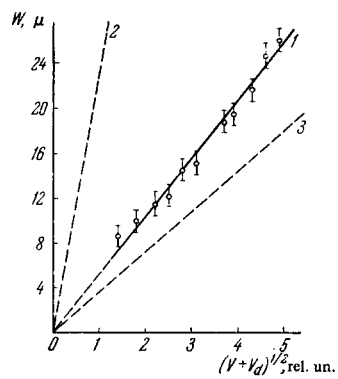

FIG. 16. Change in width of the depleted zone of a p-n junction and its dependence on the applied bias [131]. Experimental curve 1 was obtained in the investigation of an oblique section of a p-n junction. The measurements of the width of the depleted layer were conducted with the SEM operating in the secondary-emission mode. For curve 1, the concentration of the acceptor impurity N_a ($N_a = 5 \times 10^{13}$ atoms/cm^3) was determined. Curves 2 and 3 represent concentrations N_a equal to 10^{13} atoms/cm^3 and 10^{14} atoms/cm^3.

The presented method of measurement of N_a may turn out to be useful for semiconductor devices such as field-effect transistors, in which the space limitations do not allow the use of a four-point probe or other usually applied methods. It is necessary to note the limitations of the method. First, its accuracy decreases when the concentration of carriers in the semiconductor increases. Second, in certain samples, especially with very thin layers of passivated oxide, as already noted in several works,[133] electron bombardment may bring about a change in the characteristics of the device and may introduce a distortion because of the change of the surface potential on the sample. Third, the presented equation pertains to the one-dimensional geometry.

In [134a], the possibility was demonstrated of measuring the diffusion potential of a p-n junction with the aid of an SEM. The current through the junction increases sharply when the diffusion potential is balanced out by a forward bias and the dynamic resistance decreases accordingly. Theoretically, the forward current tends to infinity and the dynamic resistance tends to zero; consequently the bias potential at which the current is infinite or the dynamic resistance vanishes is equal to the diffusion potential.

In this method, the p-n junction is subjected to an exposure by a pulse of light. The induced current is measured at different bias potentials. In the region of small dynamic resistance, the induced current decreases proportionately with the dynamic resistance, and the bias potential at which the current vanishes is equal to the diffusion potential. This method is more sensitive than volt-ampere or capacitance technique; another advantage is that the electron probe can be made sufficiently thin and thus permit measurements of the local diffusion potential.

Recently,[134b] a method was described for finding the distribution of the potential in the SEM by means of an analyzer of the velocities of secondary electrons. Such a possibility develops owing to the shift of the peak of the curve of the distribution of velocities relative to the value of the local potential on the surface of the solid body. It was also shown by the authors that modification of the method makes it possible to plot by a "contactless" technique the volt-ampere characteristics of a semiconductor diode. In this case, the velocity analyzer fixes the specified potential, and the current through the p-n junction is measured in the circuit of the grounded electrode. The electron beam, comprised of secondary electrons completing the "contactless" circuit, serves as the second electrode.

Interesting possibilities are introduced by the SEM for quantitative investigations of p-n junctions, using the nature of the contrast of the image. In some cases the contrast formed by the p-n junction may depend on the second derivative of the potential at individual spots of the junction.[74] The signal from the beam of secondary electrons produced by the scanning beam was passed through an integrating network and then fed to an oscilloscope. This method allowed direct viewing of the curve of the distribution of potential in the p-n junction and a determination of its dimensions.

In a number of works, the use of the SEM was proposed for quantitative measurements of the parameters

of semiconducting crystals and elements of microcircuits. On the basis of well known potentiometric and bridge methods, it was proposed to use the SEM for the measurement of the resistance of small electric circuits.[135]

If a semiconductor crystal is illuminated by photons and if the specific resistance is not uniformly distributed, then a voltage appears between the ends of the semiconductor. This effect is called the volume photogalvanic effect. An analogous picture arises also in that case where the specimen is bombarded by electrons. The current of the beam goes through the sample, one end of which is grounded, and the potential of the opposite end is measured. The potential ΔV induced by the electron bombardment is the difference between the voltage drop formed by the current of the beam and by the potential of the ungrounded end of the specimen.[136] This effect is used for the investigation of the distribution of the specific resistance ρ_0 of the semiconductor, which can be obtained by integrating ΔV:[137]

$$\rho_0 \sim \int \frac{\partial \rho_0}{\partial x} dx \sim \int \Delta V \, dx.$$

When the diffusion length of the minority carriers is insignificant ($\sim 1\,\mu$), ΔV is measured only with difficulty. In this case, pulsed illumination of the sample has been proposed. The speed with which the study can be made (all measurements are performed within 10 sec) and the possibility of the measurement of small potential differences (of the order of several dozen mV and less) are the advantages of such a method of measurement of the distribution of potential in a crystal of germanium with nearly homogeneous conductivity.[138]

Furthermore, this method was also applied for the measurement of the distribution of the specific resistance in a semiconductor crystal.[139] Its value lies in the fact that the measurements depend on the purity of the surface of the crystal, unlike in [136,137], i.e., it becomes possible to determine the conducting regions on the surface of the sample.

b) Investigation of integrated microcircuits. The SEM offers great diagnostic possibilities in the analysis of integrated microcircuits. Higher resolution (~200 Å), significant sharpness (definition) (0.6—0.8 mm), observation of a sample without special preparation, and the possibility of observing electric and magnetic microfields—all this gives it incontrovertible advantages over optical methods. Using the effects of penetration and scattering of electrons in solids, and also the excitation by them of electron-hole pairs, it is possible to conduct quantitative measurements, inspection, and even the preparation of individual integrated circuits.

By varying the energy of the electron beam and changing by the same token the depth of its penetration, it is possible to determine the three-dimensional relief of a p-n junction in a multilayer structure.[56] The three-dimensional resolution is limited in this case by the depth of penetration of the electrons into the material.

Decreasing the dimensions of circuits makes unsuitable the use of a mechanical probe for electrical and magnetic tests. Therefore the contactless method of testing of integrated circuits by means of the SEM is of evident practical value,[56,140-142] and can serve for the determination of the general picture of the topography of the surface, of the contours of the p-n junctions that emerge to the surface, of the voltage drop across thin-film resistors, of the quality of oxide films and sputtered layers, of the quality of attachment of gold contacts, etc. The possibility is considered [142,147] of testing and selecting prepared circuits by means of an induced-current signal or a secondary-emission signal. If the obtained signal is compared with a standard signal, then the resultant error signal can be used for the automatic acceptance testing of devices.

In the works devoted to the investigation of integrated transistors of the MOST type,[127,133,144,145] an attempt is made to explain the role of inversion layers, and also the displacement of p- and n-paths at different voltages on the control electrode. The capabilities of the SEM for investigations of integrated circuits are shown in Fig. 17.[100]

A very important application of the scanning microscopes is their use in the production of individual elements of solid-state circuits. A programmed electron beam is used for the exposure of photoresists and for obtaining conductive joints.[142,147]

To control the deposition of thin films, their microtreatment, the topology and chemical composition of these films, an ion source, an SEM, and an x-ray microanalyzer were combined in a single aggregate for the production of an ion beam modulated in accord with a specified program. All operations are conducted without the transfer of the substrate from one chamber to another. The basic purpose of such an apparatus is the production of thin-film integrated circuits containing active and passive elements of micron size.

11. Stroboscopic SEM

Such an apparatus was constructed on the basis of the usual SEM for the purpose of observing fast transient processes. The image of a semiconductor device was successfully obtained at a time resolution of about 100 nsec[30]. When the SEM operates in the stroboscopic

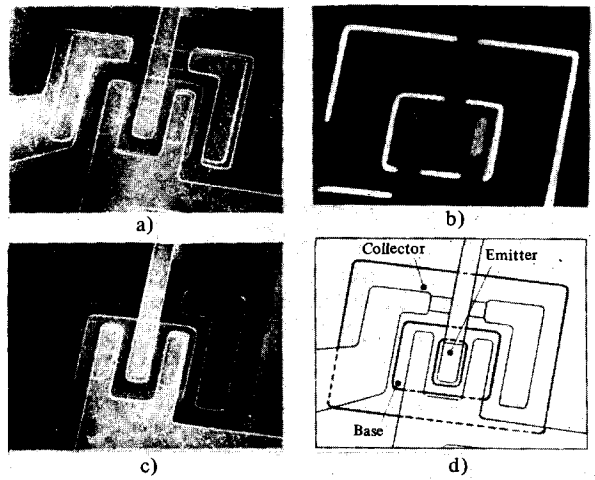

FIG. 17. Display of the structure of a transistor [100]. a) Topography in the SEM, b) change of picture upon application of an inverse voltage of 2 V, c) induced-current image upon bombardment by 10-kV electrons, d) schematic picture of the transistor.

mode, double rectangular pulses (positive and negative) are applied to the sample. The strobing pulse controlling the beam is produced by modulation with the aid of other, shorter pulses. The optimal image-construction conditions are obtained by the relation

$$f^{-1} - \tau = \frac{\delta t}{\mathscr{L}},$$

is satisfied, where τ and f are length and frequency of the pulses modulating the light, $\mathscr{L}$ and t the dimensions and time of one scanning line, and δ is the geometric resolution.

The stroboscopic principle was introduced into electron microscopy by Spivak and co-workers.[27-29] Observations with a scanning microscope are described in [30-32,146].

Figures 18a and 18b show six images of the surface of a semiconductor circuit obtained in the stroboscopic mode of operation, and in Fig. 18c shows an oscillogram of the pulsed current through the sample. In the oscillogram are shown the six corresponding positions of the stroboscopic pulses in which all six images are formed.

Plows and Nixon[31] achieved, in a stroboscopic SEM,

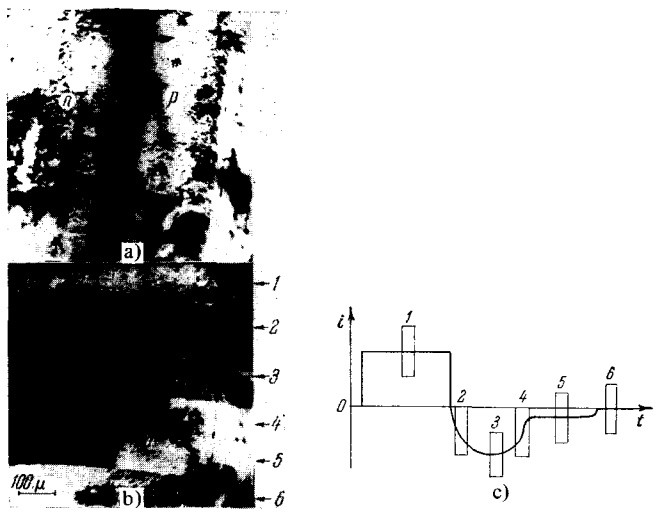

FIG. 18. Stroboscopic mode of operation of the SEM [30,37].
a) Image of semiconductor diode with applied inverse fixed bias;
b) subsequent phases of the stroboscopic image of the p-n junction,
c) oscillogram of the current through the p-n junction – six separately spaced strobing pulses corresponding to six states of the microfield on the surface of the diode.

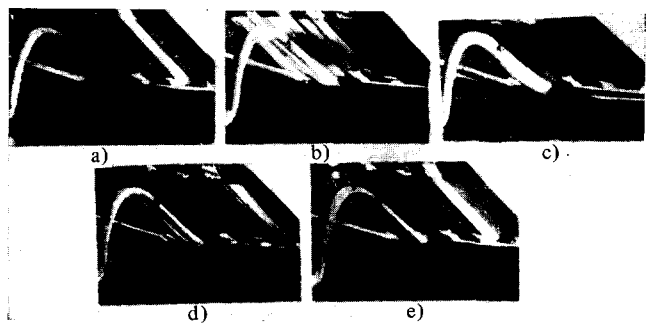

FIG. 19. Stroboscopic image of motion of a potential pulse in a solid-state circuit in different phases of the process [31]. a) $\omega t = 0$; b) $\omega t \sim \pi/2$; c) $\omega t \sim \pi$; d) $\omega t \sim 3\pi/2$; e) $\omega t \sim 2\pi$.

the possibility of analyzing transient electrical processes with good time resolution on the order of 10 nsec at an arbitrary phase of a given operating cycle (Fig. 19). According to the prognosis of the authors,[31] the time resolution of the apparatus may reach 0.1 nsec.

12. Scanning X-ray Microanalyzer*

Fruitful application of the SEM is one in which x-rays are used for the formation of the image. They are produced together with other forms of emission during the interaction of the electron beam with the specimen. The wavelength and intensity of the characteristic x-ray line emission are uniquely determined by the atomic nature of the element and the electronic structure of the atoms. In such a way, by separating some particular wavelength, it is possible to construct an image showing the distribution of a given element in the limits of the investigated area of the sample. By means of a comparison the number of x-ray quanta from the sample and from a standard analogous material, it is possible to produce a quantitative microanalysis of the substance. The resolution of such an apparatus does not exceed 1 μ, in spite of the fact that the beam may be of an even smaller diameter. This is connected with scattering processes in the solid, which induce x-ray emission from a volume of the order of 1 μ^3. At the present time, the apparatus is capable of analyzing elements from $_{11}$Na to $_{92}$U. The difficulty of the experiments with lighter elements lies in the absence of sensitive detectors for the long-wave part of the spectrum of x-ray emission. The methods being applied for the analysis of elements may be divided into two categories: a non-dispersive method (without a crystal) and a method with the application of a dispersing element. In the first, they normally use a proportional counter with a flowing gas, sufficiently sensitive to the long-wave part of the spectrum (above 5 Å), together with a pulse-height analyzer. The gas used in the counter is a mixture of 90% Ar and 10% CH_4 at a pressure of 1 atm. By this method, analyses of Be, B, C, and F were conducted successfully. With the aid of the dispersive method, based on the use of a crystal spectrometer and gas-discharge counter, it is possible to study the characteristic emission of all elements beginning with Na and ending with U, in the interval from 0.7 to 13 Å. Materials with small values of lattice constants (mica, quartz) serve as the crystal analyzer. The dispersion method may be applied also for the observation of long wave emission, but in this case it is necessary to use an analyzer crystal with a large lattice constant. For these purposes, crystals of barium stearate and lead are utilized. In such a spectrometer, the region of investigation is confined to C, N, and O. Both methods mentioned have their own advantages and disadvantages. The non-dispersive technique has high sensitivity but low resolving power. When a crystal is used the sensitivity is low but the resolving power is higher, $\Delta\lambda/\lambda = (1-5) \times 10^{-3}$ at a geometric resolution of 1 μ. The minimum quantity of material that can be studied by means of comparative microanalyzers is

*Presented in digest form.

10^{15}—10^{-16} g.[149] In the majority of cases, the x-ray microanalyzer is equipped with a collector of the secondary and absorbed electrons. In such a manner, it is possible to observe simultaneously on several tubes the image of the same sample by means of x-ray emission, secondary electrons, and absorbed electrons, or to use this apparatus only in one mode. Borovskiĭ[41b] in the USSR and Castaing[42] in France, who built a microanalyzer with a fixed beam as far back as 1951, initiated the investigations by the described method of research. Soon after, in 1957, Duncumb, working in the laboratory of Cosslett, used the principle of scanning for a microanalyzer and achieved the possibility of conducting local x-ray spectral analyses on a square of about 1 mm^2 and of seeing the distribution of various elements on the surface of the specimen.[150]

In our country, on the basis of the investigations of Kushner and co-workers,[2,3,151-157] a series of intruments was developed (RÉMP-1—RÉMP-3), in which the SEM was combined with a microanalyzer. One such instrument, manufactured by the Soviet industry (RÉMMA), is shown in Fig. 20.[185] At a resolution in the range 0.1—1 μ, this apparatus was used in the microscope made for the observation of drawn silicon p-n junctions at different biases, the structures of etched germanium, pyrophyllite, chrome pinelide, recrystallized nickel, etc. In the mode of an x-ray spectrum analyzer, the RÉMP-1 can register x-ray emission in the range from 0.7 to 10 Å, which allows the analysis of the chemical elements from Mg (Z = 12) to U (Z = 92) to be conducted. The crystal analyzer is single-crystal quartz used with focusing from the planes (1340) and (1010) and mica (001) in combination with an ionization counter of the type MSTR-4. At the present time, two modifications of the apparatus, RÉMP-2 and RÉMP-3, have been developed, with improved parameters. The latter of these is designed to have a resolution of 500 Å in the microscope mode.

An interesting application of the microanalyzer is to the study of semiconductor hetero-junctions, where an estimate of the distribution of microelements in the p-n junction becomes possible.[159a]

The development of the microanalyzer opened up the possibility of using an electron beam for obtaining x-ray patterns in a diverging beam of x-radiation (Kossel patterns[159b-c]). This new promising trend in the microanalysis of a material allows the study of imperfections of single crystals and also the exact measurement of the lattice constants.

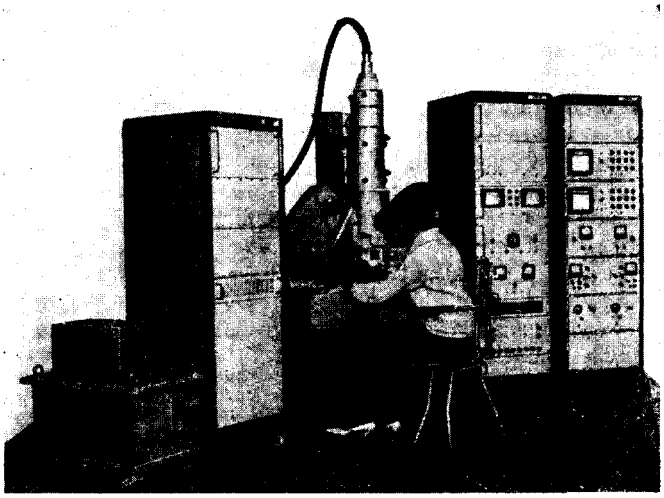

FIG. 20. SEM microanalyzer (RÉMMA) [158].

Vertsner and co-workers[160-163] developed many x-ray microanalyzers. In 1962, our industry put out the model MAR-1, with a fixed beam. The sample can be moved mechanically relative to the beam. The accelerating voltage in the apparatus is adjustable from 10 to 50 kV. In this apparatus, the quantitative analysis of elements from $_{12}$Mg to $_{92}$U from an area of 1—2 μ is possible. The following model, MAR-2, already provides for scanning the beam along the object and the use of crystal-free recording of the emission by means of flowing-gas and proportional counters.

13. Biological Applications of the SEM

The SEM in biological investigations encounters the same difficulties that faced the transmission microscope: the object-destroying influence of the vacuum and the harmful effect of the electron current. However, in comparison with the transmission microscope, the great advantage of the SEM lies in the possibility of observing massive specimens with a large depth of focus, something unattainable by other apparatus. Certain biological specimens such as tissues, blood corpuscles, bacteria, etc. after a special treatment can withstand a stay in vacuum very well, cell walls and membranes are not destroyed, and it is possible to study them with this technique. But first it is necessary to deposit a thin layer of metal of the order of 200—400 Å onto the surface of these specimens, in order to avoid the distortion of the image due to charge. The first attempts to apply the SEM for an investigation of biological specimens was described in the work of Oatley and Smith[164] in 1955. At a magnification of the order of 3000, they observed amoebae and larvae of mealy worms. The amoebae were fixed in osmic acid and on a nickel plate. To avoid charging of the surface, they covered it with a thin layer of silver.

The review of Oatley, Nixon, and Pease,[4] and the works of Washburn and Buchanan[98] describe an observation of biological specimens with exceptionally complicated surfaces. Pictures at magnifications from 300 to 20,000 were obtained of different parts of the head of the common fly, of individual cells of its eye, and the fluff of the larva of the mealy worm. Pictures of a number of interesting samples at magnifications from 300 to 18,000 were obtained by Kimoto[18] (Japan). The first pictures of fungus and molds, microstructures of the wings of a butterfly, human hair, and zinnia pollen (Fig. 21) were taken by Kimoto.

Boyde and Stewart[165,166] carried out a study of the surface of tooth enamel and the cores of teeth of man, monkey, and several rodent specimens. Before the placement of the sample into the microscope, the surface must be etched clean by 5-kV argon ions to bring out the structure, and afterwards the surface is coated with a 300 Å layer of aluminum.

In the work of Pease and Hayes,[167] the beetle

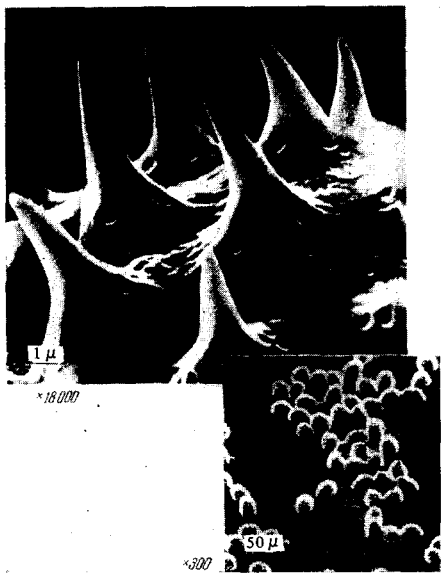

FIG. 21. Zinnia pollen at different magnifications [19].

Tribolium Confusum was chosen as the subject of investigation. Before the experiment, a test was conducted of the stability of the eggs, of the larvae, of the embryos, and of the mature beetle in vacuum of 10^{-3} Torr for a period of 30 min. Part of them withstood the tests and their further growth proceeded normally. For observations in the SEM, the time of the investigation ranged from 2 min to 1 hr. To avoid destruction of the samples by irradiation, the current of the beam at 25 kV anode potential was reduced to 2×10^{-11} A. The irradiation was constant in all experiments and comprised approximately 1% of the dose of the transmission microscope. An estimate showed that, at the conditions given above, the temperature of studied area element changes by only 0.005°C. The calculations and the experiment reported in the article showed clearly the possibility of investigating several living specimens in the SEM.

Attempts were made to investigate human tissue. The first work in this direction, albeit only at a magnification of 75 times, was made by Jague, Coalson, and Zerving.[168] In a larger article, Hayes, Pease, and MacDonald[169] describe a study of epithelial cells of the interior part of the lip and of the coronary arteries. Before placement, the specimens were washed in a sterile solution, dried, and then fixed by means of special preparations. At magnifications on the order of 5000, it was possible to distinguish bacteria on the surface of the epithelium. On the endothelial layer of the coronary arteries at, magnifications of 3000 times, the red blood cells were well distinguished. Experiments on the observation of cathode luminescence caused by the electron beam were also carried out on biological materials.[168] Owing to the possibility of obtaining three-dimensional images in [170], the three-dimensional structures of the elements of blood, plasma, etc. were successfully shown (Fig. 22). In conclusion, let us stop on the discussion of SEM problems at the All-European Electron Microscopy Congress held in September of 1968 in Rome.[171]

FIG. 22. Plasma and red blood cells (indicated by arrows), ×6700 [170].

The concluding reports of this congress can be divided into three groups: 1) high-voltage scanning microscopy, 2) theory and experiment regarding the nature of contrast, and 3) new applications.

1. Smith and co-workers called attention to the fact that high-voltage apparatus operating "in transmission" possesses an essential advantage in comparison with the usual transmission electron microscope; the former has less chromatic aberration, makes it easy to carry out a velocity analysis of the electrons passing through the sample, making it possible to obtain an image "in light" of electrons of different velocities. Stroinik and Cowley describe a 600 kV SEM, also operating "in transmission," and reach the same conclusions. Crewe and co-workers describe the relatively simple model of the apparatus with an autoelectronic emitter, and report a resolution of 20 Å "in transmission." This result appears to be a record in a scanning microscope. The authors call attention to the fact that the theoretically anticipated resolution should be of the order of 5 Å, which represents the resolution of a high-grade transmission microscope.

2. The reports of Nixon et al. and Spivak et al. were concerned with the questions of the stroboscopic scanning electron microscope and the problem of contrast of electric and magnetic microfields. The report[30] at the All-union Conference on Electron Microscopy in July 1967 was concerned with the review of the problems of the stroboscopic electron microscope, including the scanning electron microscope. These questions were raised again because the stroboscopic electron microscope significantly expands the possibilities of studying rapid processes, particularly in semiconductor devices, in microelectronics, etc. In the work of another group of investigators, the variety of the forms of contrast of p-n junctions (six types of contrast) are described and a theory explaining their formation is given. Reimar performed a measurement of the current of electrons forming the contrast, and called attention to the fact that not only the contrast is formed at the site of the contact of the electron beam and the specimen, but also there is an essential influence of the secondary-electron current, which is scattered by the walls of the specimen chamber that forms a supplemental background to the picture. A number of short remarks on the mechanism of formation of contrast of electric microfields was made by Kimoto.

3. Among the new applications of scanning optics, mention should be made of the work of Bigan and Sella, who demonstrated high-grade images of the domain structure of ferroelectrics.

The possibility of obtaining images of samples of arbitrary shape and differently oriented to the beam of charged particles, and moreover with a large depth of focus, opens up many opportunities to study the three-dimensional structure of bodies. The variety of physical phenomena, particularly of local x-ray emission, which serve to form the video signal, open up great prospects of furthering the expansion of the fields of application of the scanning microscope. High sensitivity to electric and magnetic microfields as applied to semiconductors and microelectronic devices allows the study of these samples under an insulating layer without destroying them. An understanding of the nature of the contrast in the formation of the image leads to the development of quantitative scanning microscopy. The reduction of the errors of the apparatus brings its geometrical resolution close to the potential resolution of a high-grade transmission microscope.

The apparatus can obtain stable images of rapidly occurring phenomena of periodic nature, with a time resolution of tenths of a nanosecond.[146] There is no doubt that the scanning electron microscope, in which the principles of electron optics and radiophysics are combined, will be perfected further and extend the range of applications.

Note added in proof: The applications of the SEM were considered recently at symposia in the USA [172].

[1] U. M. Kushner, PTÉ No. 4, 3 (1958).
[2] U. M. Kushner, Radioteknika i Élektronika 5, 74 (1962).
[3] Elektronnaya mikroskopiya (Electron Microscopy), A. A. Lebedev, ed., Gostekhizdat, 1954.
[4] C. W. Oatley, W. C. Nixon, and R. F. W. Pease, Advances in Electronics and Electron Phys. 21, 181 (1965).
[5] P. R. Thornton, Scanning Electron Microscopy, Chapman and Hall, London, 1968.
[6] M. Knoll, Zs. techn. Phys. 16, 767 (1935).
[7] M. Knoll and R. Thsill, Zs. Phys. 113, 260 (1939).
[8] M. Ardenne, Zs. Phys. 109, 553 (1938).
[9] M. Ardenne, Zs. Phys. 109, 407 (1938).
[10] M. Ardenne, Zs. techn. Phys. 20, 334 (1939).
[11] V. K. Zworykin and J. Hiller, ASTM Bull. 117, 15 (1942).
[12] F. Davoine, These (Lyon, 1957).
[13] C. Brachet, Bull. Assoc. Tech. Martime Aeron. 45, 369 (1946).
[14] R. F. W. Pease and W. C. Nixon, J. Sci. Instrum. 42, 81 (1965).
[15] D. McMullan, Proc. IEE 100, pt. 11, 245 (1953).
[16] A. D. G. Stewart and M. A. Snelling, Proc. 3rd ERCEM, Prague, vol. A., 1964, p. 55.
[17] Cambridge Instrument Company, Stereoscan, catalogues.
[18] S. Kimoto, Hachimoto, and H. Sato, Proc. 6th ICEM, Kyoto, vol. A, 1966, p. 197.
[19] Advertisements of "Cambridge Instrument Company," and "Stereoscan."
[20] H. Kimura, H. Higuchi, H. Tamura, and M. Maki, see [18], p. 195: J. Electron Microscopy 15, 21 (1966).
[21] A. Rose, Advances in Electronics and Electron Phys. 1, 131 (1948).
[22] T. E. Everhart, Thesis (Cambridge University, 1957).
[23] R. F. W. Pease, Thesis (Cambridge University, 1964).
[24] D. B. Langmuir, Proc. IEE 25, 977 (1937).
[25] M. E. Haine and P. A. Einstein, Brit. J. Appl. Phys. 3, 40 (1952).
[26] K. C. A. Smith, Thesis (Cambridge University, 1956).
[27] G. V. Spivak, V. G. Dyukov, N. N. Sedov, and A. N. Nevzorov, Izv. AN SSSR, ser. fiz. 30, 742 (1966): also in [18], p. 215.
[28] A. E. Luk'yanor, and G. V. Spivak, see [18], p. 611; G. V. Spivak and A. E. Luk'yanov, Izv. AN SSSR ser. fiz. 30, 781 (1966).
[29] G. V. Spivak, V. I. Petrov, and O. P. Pavlyuchenko, Izv. AN SSSR, ser. fiz. 30, 793 (1966).
[30] G. V. Spivak, E. M. Dubinina, G. V. Saparin, et al., ibid. 32(7), 1098 (1968)—report at plenary session of VI All-union Conference on Electron Microscopy (Novosibirsk, 11–16 July 1967).
[31] G. P. Plows and W. C. Nixon, J. Sci. Instrum. ser. 2, 1, 595 (1968).
[32] a) G. V. Spivak, G. V. Saparin, et al., Proc. 4th ERCEM, Rome, 1968, vol. 1, p. 89. b) R. S. Gvosdover, G. V. Spivak, A. E. Lukianov, M. V. Bikov, and G. V. Saparin, Proc. 4th Nat. Conference on Electron Microprobe Analysis (Pasadena, USA), University of Southern California, 1969, p. 58.
[33] R. F. M. Thornley, Thesis (Cambridge University, 1960).
[34] R. F. M. Thornley, Proc. 2nd ERCEM, Delft, vol. 1, 1960, p. 173.
[35] V. N. Vertsner and J. B. Chentsov, Izv. AN SSSR, ser. fiz. 24, 519 (1959); PTÉ No. 5, 180 (1963).
[36] a) G. V. Spivak, I. N. Prilezhaeva, and V. K. Azovtsev, Dokl. Akad. Nauk SSSR 105, 965 (1955), b) W. C. Nixon, Proc. Symp. Electron Beam Techniques for Microelectronics and Reliability (RRE Malvern, 1964), vol. 4, Oxford, Pergamon Press, 1965, p. 16. c) R. S. Paden and W. C. Nixon, J. Sci. Instrum., Ser. 2, 1, 1073 (1968).
[37] G. Mollenstedt and F. Lenz, Advances in Electronics and Electron Phys. 18, 251 (1963).
[38] G. V. Spivak and G. V. Saparin, Izv. AN SSSR, ser. fiz. 30, 761 (1966).
[39] I. W. Drummond and I. V. P. Long, Nature 215, 951 (1967).
[40] M. Gabbay, R. Contte, C. Guilland, and C. Monllor, Compt. rend. 261, 3325 (1965).
[41] a) V. E. Yurasova, G. V. Spivak, and A. I. Krokhina, in: Katodnoe raspylenie kak metod preparirovaniya v élektronnoĭ mikroskopii (Cathode Sputtering as a Method of Preparation in Electron Microscopy), M. NTO A. S. Popov, 1965, p. 54, b) I. B. Borovskiĭ, in Problemy metallurgii, Akademiku N. P. Pardiny K 70-letiyu (Problems of Metallurgy, dedicated to Academician I. P. Bardin on his 70th birthday), AN SSSR 1953, p. 153.
[42] a) R. Castaing, Theses (Universite de Paris, 1951). b) R. Castaing and A. Guinier, Anal. de chem. 25, 724 (1953).
[43] R. Castaing and J. Descamps, J. Phys. et radium

16, 304 (1955).
[44] R. Castaing, Advances in Electronics and Electron Phys. 13, 317 (1960).
[45] A. V. Grewe, Scanning Electron Microscope, Pat. USA No. 3191028, 250–49 5; 22.06.65.
[46] A. V. Grewe, J. Appl. Phys. 35, 3075 (1965).
[47] A. V. Grewe, see [18], p. 625.
[48] A. V. Grewe, see [18], p. 627.
[49] A. V. Grewe, see [18], p. 629.
[50] A. V. Grewe, see [18], p. 631.
[51] T. E. Everhart, C. W. Oatley, and O. C. Wells, J. Electron. and Control 7, 97 (1959).
[52] E. I. Sternglass, Phys. Rev. 95, 345 (1954).
[53] P. Palluel, Compt. rend. 223, 1492, 1551 (1947).
[54] S. Kimoto, Direct Observation of Silicon p-n Junction with Scanning Electron Microscope, "JEOL," 1965.
[55] E. Wainryb and J. Philliber, see [16], p. 53.
[56] T. E. Everhart, O. C. Wells, and R. K. Matta, J. Electrochem. Soc. 111, 929 (1962).
[57] P. Pinard, Theses (Lyon, 1964).
[58] D. B. Wittry and D. F. Kyser, J. Appl. Phys. 35, 2439 (1964).
[59] a) D. B. Wittry and D. F. Kyser, J. Appl. Phys. 36, 1387 (1965). b) Yu. P. Demidov and R. P. Gurova, Fiz. Tekh. Poluprov. 1, 1235 (1967) [Sov. Phys.-Semicond. 1, 1030 (1968)].
[60] D. B. Wittry, see [18], p. 607.
[61] J. M. Kushner, Fizicheskiĭ Éntsiklopedicheskii Slovar', (Encyclop. Dict. of Physics) Vol. 5, Sov. Entsiklopediya, 1966, p. 494.
[62] C. M. Oatley and T. E. Everhart, J. Electron. and Control 2, 568 (1957).
[63] J. R. Banbury and W. C. Nixon, J. Sci. Instrum. 44, 889 (1967).
[64] G. V. Spivak, G. V. Saparin, N. N. Sedov, J. F. Komolova, et al., Izv. AN SSSR, ser. fiz. 32, 962, 967 (1968).
[65] W. Czaja and G. N. Wheatley, J. Appl. Phys. 35, 2782 (1964).
[66] W. Czaja and I. R. Patel, J. Appl. Phys. 36, 1477 (1965).
[67] G. V. Spivak, G. V. Saparin, A. E. Yunovich, M. K. Antoshin, et al., Fiz. Tekh. Poluprov 2(12) 1791 (1968) [Sov. Phys.-Semicond. 2, 1492 (1969)].
[68] See [41b], p. 135.
[69] Catalog of the firm "Cambridge Instrument Company, Ltd.," 1961, "Microscan X-Ray Analyzer."
[70] R. Castaing and G. Slodsian, see [34], p. 169.
[71] a) G. V. Saparin, G. V. Spivak, N. N. Sedov, and L. F. Komolova, Izv. AN SSSR, ser. fiz. 32, 947 (1968): G. V. Saparin, G. V. Spivak, N. N. Sedov, and L. F. Comolova, see [32], p. 87. b) G. V. Saparin, Dissertation (MGU, Dept. of Physics, 1967).
[72] G. V. Spivak et al., Izv. AN SSSR, ser. fiz. 27, 1139 (1963).
[73] G. V. Spivak, G. V. Saparin, B. Massarani, and M. V. Bikov, see [16], p. 285.
[74] G. V. Spivak, G. V. Saparin, and N. A. Pereverzev, Izv. AN SSSR ser. fiz. 26, 1339 (1962).
[75] G. V. Spivak, N. G. Kanavina, I. N. Chernyshev, and I. S. Spitnikova, Dokl. Akad. Nauk SSSR 92, 541 (1953).
[76] G. V. Spivak et al., ibid. 105, 965 (1955).
[77] I. M. Gelfand and G. E. Shilov, Teoriya obobshchennykh funktsiĭ (Theory of Generalized Functions), Ch. 1, M. Fizmatiz, 1959.
[78] In: Vychislitel'nye metody i programirovanie (Calculating Methods and Programming) No. 8, M.G.U. 1968.
[79] N. N. Sedov, G. V. Spivak, G. V. Saparin, and V. G. Galstyan, Radiotekhnika i Élektronika 13, 2278 (1968).
[80] G. V. Spivak and V. I. Ljubchenko, Izv. AN SSSR ser. fiz. 23, 627 (1959).
[81] G. V. Spivak, G. V. Saparin, G. V. Spezhnev, and N. N. Pesotskiĭ, Izv. AN SSSR ser. fiz. 32, 967 (1968).
[82] G. V. Spivak, G. V. Saparin, and S. S. Stepanov, ibid. 30, 881 (1966).
[83] G. V. Spivak, G. V. Saparin, and N. N. Sedov, ibid. 32, 962 (1968).
[84] G. V. Saparin, G. V. Spivak, and S. S. Tepanov, see [18], p. 609.
[85] S. Kimoto, H. Hashimoto, and T. Suganuma, Electron Microprobe Symposium (Washington, October 13, 1964).
[86] K. C. A. Smith, see [34], p. 177.
[87] K. C. A. Smith, Encyclopedia of Electron Microscopy (Reinhold Clark, Ed.) New York, 1961.
[88] A. D. G. Stewart, Proc. 5th ICEM, Philadelphia, 1962, D12–D13.
[89] O. C. Wells, Brit. J. Appl. Phys. 11, 199 (1960).
[90] C. F. Tipper, D. L. Dagg, and O. C. Wells, J. Iron and Steel 139, 133 (1959).
[91] L. Cartz and R. Thornley, J. Amer. Ceram. Soc. 45, 425 (1962).
[92] S. Chatterji and I. W. Jeffery, J. Amer. Ceram. Soc. 46, 187 (1963).
[93] S. Chatterji and I. W. Jeffery, Nature 209, 1233 (1966).
[94] G. V. Saparin and G. V. Spivak, Izv. AN SSSR ser. fiz. 30, 787 (1966).
[95] K. C. A. Smith and C. W. Oatley, Brit. J. Appl. Phys. 6, 391 (1955).
[96] K. C. A. Smith and C. W. Oatley, Brit. J. Appl. Phys. 2, 90 (1956).
[97] K. C. A. Smith, Pulp Paper Mag. (Canad.), Techn., Sec. 60, T366 (1959).
[98] O. V. Washburn and I. G. Buchanan, Pulp Paper Mag. (Canad.) 65, 400 (1964).
[99] M. J. Culpin and F. Dunderal, see [16], p. 421.
[100] "JEOL," Application of JSM-2 Scanning Electron Microscope, 1968.
[101] F. Davoine, B. Bernard, and P. Pinard, see [34], p. 165.
[102] F. Davoine, R. Gauthier, and A. Nouailhalt, Microsc. J. 2, 135 (1963).
[103] F. Davoine, P. Pinard, and A. Nouailhalt, Microsc. J. 2, 93 (1963).
[104] F. Davoine and P. Pinard, see [16], p. 113.
[105] F. Davoine, P. Pinard, and M. Martineau, J. Phys. et radium 21, 121 (1960).
[106] S. Shirai, A. Onoguchi, and T. Ichinokawa, see [18], p. 199.
[107] E. Weinryb and J. Philliber, see [16], p. 53.
[108] J. H. L. McAuslan and K. C. A. Smith, Proc. ICEM, Stockholm, 1957, p 343.
[109] R. F. W. Pease and R. A. Ploc, Trans. Met. Soc. of Aime 233, 1949 (1965).

[110] R. F. W. Pease, A. N. Brocra, and R. A. Ploc, see [16], p. 389.
[111] A. D. G. Stewart and A. Boyde, Nature 196, 81 (1962).
[112] J. T. McGrath, J. G. Buchanan, and R. C. A. Thurston, J. Inst. Metals 91, 34, 104 (1962).
[113] J. Minkoff and W. C. Nixon, J. Appl. Phys. 37, 4848 (1966).
[114] J. W. Allen and K. C. A. Smith, J. Microelectronics 1, 439 (1965).
[115] I. G. Davies, K. A. Hughes, D. V. Sulway, and P. R. Thornton, Solid-State Electronics 9, 275 (1966).
[116] a) J. J. Lander, Appl. Phys. Lett. 3, 206 (1963). b) J. D. Cross and P. M. Cross, J. Sci. Instrum., Ser. 2, 1, 1123 (1968).
[117] A. H. W. Beck and H. J. Ahmed, J. Electron. and Control 14, 997 (1962).
[118] G. A. Haas and R. E. Thomas, J. Appl. Phys. 34, 3457 (1963).
[119] G. A. Haas and R. E. Thomas, Surface Sci. 4, 64 (1966).
[120] C. W. Oatley, New Scientist 153, 12 (1958).
[121] I. W. Drummond and P. R. Thornton, see [16], p. 287.
[122] P. R. Thornton, M. J. Culpin, and I. W. Drummond, Solid-State Electronics 8, 532 (1963).
[123] D. A. Show, K. A. Hughes, N. F. B. Neve, D. V. Sulvey, and P. R. Thornton, Solid-State Electronics 9, 664 (1966).
[124] N. F. B. Neve, K. A. Hughes, and P. R. Thornton, J. Appl. Phys. 37, 1704 (1966).
[125] H. F. B. Neve, K. A. Hughes, and P. R. Thornton, IEEE Trans. on Electron Devices ED-13 (8/9), 639 (1966).
[126] H. Higuchi and H. Tamura, Japan J. Appl. Phys. 4, 316 (1965).
[127] H. Higuchi and H. Tamura, Japan J. Appl. Phys. 4, 1021 (1965).
[128] H. Kimura, H. Higuchi, H. Tamura, and M. Maki, see [18], p. 195.
[129] P. R. Thornton, K. A. Hughes et al., Microelectronics and Reliability 5, 291 (1966).
[130] C. Munakata, Japan J. Appl. Phys. 5, 249 (1966).
[131] N. C. McDonald and T. E. Everhart, Appl. Phys. Lett. 7, 267 (1965).
[132] P. R. Thornton and N. F. B. Neve, Microelectronics and Reliability 5, 299 (1966).
[133] D. Green, I. E. Sanclol, et al., Appl. Phys. Lett. 6, 3 (1965).
[134] a) C. Munakata, Japan J. Appl. Phys. 6, 274 (1967). b) O. C. Wells, C. G. Bremer, J. Sci. Instrum., Ser. 2, 1, 902 (1968).
[135] R. Watanabe and C. Munakata, Japan J. Appl. 4, 200 (1965).
[136] C. Munakata, Japan J. Appl. Phys. 4, 697 (1965).
[137] C. Munakata, Japan. J. Appl. Phys. 4, 815 (1965).
[138] C. Munkata, Japan J. Appl. Phys. 6, 548 (1967).
[139] C. Munakata, J. Sci. Instrum. (J. Phys. E) 1 (ser. 2), 639 (1968).
[140] T. E. Everhart, A. I. Gonzales, P. H. Hoff, and N. C. McDonald, see [18], p. 20.
[141] R. F. M. Thornley and J. D. Hutchison, Appl. Phys. Lett. 13, 249 (1968).
[142] J. M. Mackintosh, Proceed. of IEEE 53, 426 (1965).
[143] A. N. Broers, Rev. Sci. Instrum. 40, 1040 (1969).
[144] D. V. Sulvey, K. A. Hughes, V. A. Evans, and P. R. Thornton, Appl. Phys. Lett. 8, 296 (1966).
[145] D. Green and H. C. Nathanson, Proc. IEEE 53, 183 (1965).
[146] G. Y. Robinson, R. M. White, and N. C. McDonald, Appl. Phys. Lett. 13, 407 (1969).
[147] J. W. Thornhill and J. M. Mackintosh, Microelectronics and Reliability 4, 97 (1965).
[148] G. S. Glinski, T. S. Noussean, and W. R. Samaroc, Proc. IEEE 52, 1900 (1964).
[149] V. E. Cosslett, see [18], p. 11.
[150] G. Duncumb, Thesis (Cambridge University, 1957).
[151] Yu. M. Kushnir, see [61], p. 497.
[152] Yu. M. Kushnir et al., Izv. AN SSSR ser. fiz. 25, 695 (1961).
[153] Yu. M. Kushnir et al., Zavodskaya Laboratoriya 27, 1528 (1961).
[154] Yu. M. Kushnir et al., Izv. AN SSSR ser. fiz. 27, 415 (1963).
[155] Yu. M. Kushnir et al., ibid. 27, 1166 (1963).
[156] Yu. M. Kushnir et al., Zavodskaya Laboratoriya 30, 1510 (1964).
[157] D. V. Fetisov, Yu. M. Kushnir, S. A. Ditsman, et al., Izv. AN SSSR ser. fiz. 32, 942 (1968).
[158] Suma Factory of Electron Microscopes and Electronic Automation Apparatus, Description of apparatus "RÉMMA," 1968.
[159] a) S. A. Ditsman, T. A. Kupriyanova, O. D. Prokhorova, and A. T. Glazernov, Izv. AN SSSR ser. fiz. 32, 953 (1968), b) W. Kossell, Nachr. Acad. Wiss. Gottingen, Math.-Phys. Kl. 1, 11, 229 (1935); L. S. Birks, Rentgenovskiĭ analiz s pomoshch'yu elektronnogo zonda (X-Ray Microanalysis by Means of an Electron Probe), Metallurgiya, 1966.
[160] L. N. Malakhov, V. N. Vertsner, and A. A. Lebedev, Izv. AN SSSR ser. fiz. 23, 770 (1959).
[161] V. N. Vertsner and L. N. Malachov, Dokl. Akad. Nauk SSSR 118, 266 (1958) [Sov. Phys.-Dokl. 3, 86 (1958)].
[162] V. N. Vertsner, J. V. Vorobyev, L. N. Malachov, Fiz. Tverd Tela 2, 109 (1959) [Sov. Phys.-Solid State 2, 99 (1959)].
[163] V. N. Vertsner, R. I. Lomunov, and J. V. Chentsov, Izv. AN USSR, ser. fiz. 30, 778 (1965).
[164] C. W. Oatley and K. C. A. Smith, Brit. J. Appl. Phys. 6, 391 (1955).
[165] A. Boyde and A. D. G. Stewart, J. Ultra Structure Research 7, 159 (1962).
[166] A. Boyde and A. D. G. Stewart, Nature 198, 1102 (1963).
[167] P. F. W. Pease and T. L. Hayes, Nature 210, 1049 (1966).
[168] W. E. Jague, J. Coalson, and A. Zerving, Exp. Molec. Path. 4, 576 (1965).
[169] T. L. Hayes and R. F. M. Pease, et al., Lab Investigation 15, 1320 (1966).
[170] J. A. Clarke, A. J. Salisbury, and F. R. Rowland, Science J. (London 4(8), 54 (1968).
[171] See [32a], p. 67.
[172] Proc. 1th (May 1968) and 2nd (May 1969) Sympos. SEM (Om Johari, Ed.), Chicago, IIT Research Inst.; Proc. 4th Nat. Conf. on Electron Microprobe Analysis (July 1969), University of South. California.

Translated by M. Richman